Elsevier Editorial System(tm) for Journal of Allergy and Clinical Immunology: In Practice
Manuscript Draft

Manuscript Number: INPRACTICE-D-16-00040R2

Title: Precision molecular diagnosis defines specific therapy in combined immunodeficiency with megaloblastic anaemia secondary to MTHFD1 deficiency

Article Type: Original Article

Section/Category: Immune Deficiencies, Infection, and Systemic Immune Disorders

Keywords: Megaloblastic anemia; C-1-tetrahydrofolate synthase, cytoplasmic (C1-THF synthase); Folinic acid; Combined Immunodeficiency; Lymphopenia

Corresponding Author: Prof. Saul N. Faust, MBBS FRCPCH PhD FHEA

Corresponding Author's Institution: University of Southampton

First Author: Kesava A Ramakrishnan, MD

Order of Authors: Kesava A Ramakrishnan, MD; Reuben J Pengelly, MBiol; Yifang Gao , PhD; Mary Morgan, FRCPath; Sanjay V Patel, MRCPCH; Graham Davies , FRCPCH; Sarah Ennis, PhD; Saul N. Faust, MBBS FRCPCH PhD FHEA; Anthony P Williams, PhD FRCPath

Manuscript Region of Origin: UNITED KINGDOM

Abstract: Background: Methylenetetrahydrofolate dehydrogenase (MTHFD1) deficiency has recently been reported to cause a folate responsive syndrome displaying a phenotype that includes megaloblastic anemia and severe combined immunodeficiency (SCID).
Objective: To describe our investigative approach to the molecular diagnosis and evaluation of immune dysfunction in a family with MTHFD1 deficiency.
Methods: Exome sequencing and analysis of variants in genes involved in the folate metabolic pathway in a family with two affected siblings. Routine laboratory and research data were analyzed to gain an in depth understanding of innate, humoral and cell mediated immune function before and after folinic acid supplementation.
Results: Interrogation of exome data for concordant variants between the siblings in the genes involved in folate metabolic pathway identified a heterozygous mutation in exon 3 of the MTHFD1 gene that was shared with their mother.

In view of highly suggestive phenotype, we extended our bioinformatics interrogation for structural variants in the MTHFD1 gene by manual evaluation of the exome data for sequence depth coverage of all the exons. A deletion involving exon 13 that was shared with their father was identified.

Routine laboratory data showed lymphopenia involving all subsets and poor response to vaccines. In-vitro analysis of dendritic cell and lymphocyte function were comparable to healthy volunteers. Treatment with

folinic acid led to immune reconstitution enabling discontinuation of all prophylactic therapies.
Conclusion: Exome sequencing demonstrated MTHFD1 deficiency as a novel cause of a combined immunodeficiency. Folinic acid was established as precision therapy to reverse the clinical and laboratory phenotype of this primary immunodeficiency.

Medicine

UNIVERSITY OF Southampton

JACI: In Practice Editorial Office
University of Iowa Hospitals & Clinics
Iowa City, IA, 52242
Phone 319-356-7739
Fax 319-467-7583
Email: inpractice@aaaai.org

6th July 2016

Dear Deputy Editor,

RE: Precision molecular diagnosis defines specific therapy in combined immunodeficiency with megaloblastic anaemia secondary to *MTHFD1* deficiency.

Many thanks for your kind email and provisional acceptance of our paper.

We have

a) reinserted lines lines 383-386 back into the manscript.

b) moved the Online Repository figure legends to the end of the repository text file.

We will email all CoI forms as soon as we have them from all authors but have not delayed this re-submission.

Yours sincerely,

Saul N. Faust
Professor in Paediatric Infectious Disease and Immunology
s.faust@soton.ac.uk

Anthony P. Williams
Professor in Translational Medicine
apw2@soton.ac.uk

TITLE PAGE

Title

Precision molecular diagnosis defines specific therapy in combined immunodeficiency with megaloblastic anaemia secondary to *MTHFD1* deficiency.

Concise title

Combined immunodeficiency caused by *MTHFD1* deficiency

Authors

Kesava A. Ramakrishnan MD[1*], Reuben J. Pengelly PhD[3*], Yifang Gao PhD[2], Mary Morgan FRCPath[4], Sanjay V. Patel MD[4], Graham Davies MD[5], Sarah Ennis PhD[3], Saul N. Faust MD, PhD[1,4], Anthony P. Williams MD, PhD[2,6]

Affiliations

[1]Academic Unit of Clinical and Experimental Sciences, Faculty of Medicine and Institute for Life Sciences, University of Southampton and NIHR Biomedical Respiratory Unit, University Hospital Southampton NHS Foundation Trust, Southampton, UK.

[2]Academic Unit of Cancer Sciences, Faculty of Medicine and Institute for Life Sciences, University of Southampton, and CRUK NIHR Experimental Cancer Medicine Centre

[3]Academic Unit of Human Development and Health, Human Genetics and Genomic Medicine, Faculty of Medicine, University of Southampton, Southampton, UK.

[4]Southampton NIHR Wellcome Trust Clinical Research Facility and Department of Paediatric Medicine, University Hospital Southampton NHS Foundation Trust, Southampton, UK.

[5]Department of Paediatric Immunology, Great Ormond Street Hospital for Children NHS Foundation Trust, London, UK.

[6]Department of Allergy, Asthma and Clinical Immunology, University Hospital Southampton NHS Foundation Trust, Southampton, UK.

*** These authors contributed equally.**

Contact for Correspondence

Professor Saul Faust

Southampton NIHR Wellcome Trust Clinical Research Facility, Mailpoint 218, University Hospital Southampton NHS Foundation Trust, Southampton, SO16 6YD, UK.

Tel: 023 8120 4939

Fax: 023 8120 5023

E Mail: S.Faust@soton.ac.uk

Word Count

Abstract - 143

Text – ~~2808~~2849

Number of figures – 2

Number of references - 17

Key Words

Megaloblastic anemia

C-1-tetrahydrofolate synthase, cytoplasmic (C1-THF synthase)

Folinic acid

Combined Immunodeficiency

Lymphopenia

Abbreviations

MTHFD1 – Methylenetetrahydrofolate dehydrogenase 1

SCID – Severe combined immunodeficiency

PCP - *Pneumocystic jirovecii* pneumonia

TRECs - T-cell receptor excision circles

PBMCs - Peripheral blood mononuclear cells

TH1 – T helper 1

TH17 – T helper 17

cDNA – Complementary DNA

PCR – Polymerase chain reaction

TCR – T cell receptor

CD_{XX} – Cluster of differentiation molecule

Anti-CD_{XX} – Monoclonal antibody to CD_{XX}

IFNγ – Interferon γ

IL-17 – Interleukin 17

WES – Whole exome sequencing

WGS – Whole genome sequencing

Highlights

1. What is already known about this topic? Recessively inherited MTHFD1 deficiency has previously been described to present with a severe combined immunodeficiency
2. What does this article add to our knowledge? Exome sequencing demonstrated *MTHFD1* deficiency as a novel cause of a combined immunodeficiency and folinic acid was established as precision therapy to reverse the clinical and laboratory phenotype.
3. How does this study impact current management guidelines? Early use of new molecular diagnostic techniques can personalise treatment in managing unexplained immunodeficiencies and in some cases prevent the need for bone marrow transplantation.

Abstract

Background: Methylenetetrahydrofolate dehydrogenase *(MTHFD1)* deficiency has recently been reported to cause a folate responsive syndrome displaying a phenotype that includes megaloblastic anemia and severe combined immunodeficiency (SCID).

Objective: To describe our investigative approach to the molecular diagnosis and evaluation of immune dysfunction in a family with *MTHFD1* deficiency.

Methods: Exome sequencing and analysis of variants in genes involved in the folate metabolic pathway in a family with two affected siblings. Routine laboratory and research data were analyzed to gain an in depth understanding of innate, humoral and cell mediated immune function before and after folinic acid supplementation.

Results: Interrogation of exome data for concordant variants between the siblings in the genes involved in folate metabolic pathway identified a heterozygous mutation in exon 3 of the MTHFD1 gene that was shared with their mother.

In view of highly suggestive phenotype, we extended our bioinformatics interrogation for structural variants in the MTHFD1 gene by manual evaluation of the exome data for sequence depth coverage of all the exons. A deletion involving exon 13 that was shared with their father was identified.

Routine laboratory data showed lymphopenia involving all subsets and poor response to vaccines. In-vitro analysis of dendritic cell and lymphocyte function were comparable to healthy volunteers. Treatment with folinic acid led to immune reconstitution enabling discontinuation of all prophylactic therapies.

Conclusion: Exome sequencing demonstrated *MTHFD1* deficiency as a novel cause of a combined immunodeficiency. Folinic acid was established as precision therapy to reverse the clinical and laboratory phenotype of this primary immunodeficiency.

Introduction

Derivatives of folic acid play a critical role in cellular one carbon metabolism, acting as donors and recipients of one-carbon units involved in synthesis and breakdown of amino acids as well as in the synthesis of thymidine and purines (1). C-1-tetrahydrofolate synthase (C1-THF synthase) is a cytoplasmic tri-functional enzyme essential for processing single carbon folate derivatives, encoded by the gene methylenetetrahydrofolate dehydrogenase *(MTHFD1)*. Mutations in *MTHFD1* have previously been reported to cause a syndrome displaying megaloblastic anemia, severe combined immunodeficiency (SCID), mild mental retardation and treatment-refractory epilepsy that was responsive to metabolic supplementation (2, 3). Four further case reports (4), two whom died of overwhelming sepsis have extended the phenotype to include atypical hemolytic uremic syndrome, microangiopathy and retinopathy. We present the long term follow up data of a family with two siblings who carry novel compound heterozygous mutations in the *MTHFD1* gene. Specifically, we have characterized the immune function in more detail and documented the response in immune function to folinic acid supplementation.

Methods

Subjects: Two brothers born to a mother of Southeast Asian and father of Caucasian origin managed in our specialist immunology service for more than a decade. Consent for research investigations was obtained (NHS Research Ethics 09/H502/4).

Exome Sequencing: Exome enrichment was performed using the SureSelect Human All Exon V4.0 kit (Agilent), prior to sequencing on the Illumina HiSeq 2000 system. Following sequencing, data processing was performed as previously described (5).

PCR amplification: PCR was performed according to manufacturer instruction using a Phusion high-fidelity PCR kit from Thermo Scientific. PCR conditions and primer sequences used for amplification exons 3 and 13 are summarized in table S1 in the online repository.

RNA amplification: RNA was extracted from lithium heparin anti-coagulated whole blood using QIAamp RNA Blood Mini Kit (Qiagen Uk). 200 ng of total RNA was reverse transcribed and cDNA amplified using MTHFD1 gene specific primers (cDNAF and cDNAR) as per manufacturer instructions using SuperScript™ III One-Step RT-PCR System (Life technologies).

Flow cytometry: A two step staining process for surface and intracellular antigens was performed according to manufacturer instructions using BD fix-perm kit. Flow cytometry data were acquired on a BD FACS canto II. At least 200,000 events were collected for lymphocyte assays and 500,000 for the dendritic cell assays. Data were analyzed using FACS Diva software and gating strategy is illustrated in the supplementary figures 1 & 2.

Results

Clinical manifestations

The elder sibling (patient A) presented at 4 months of age with clinical and radiological features consistent with *Pneumocystic jirovecii* pneumonia (PCP). SCID was diagnosed on the basis of susceptibility to PCP and severe lymphopenia involving all lymphoid subsets. Subsequent investigations found no mutations in the genes known to cause SCID at that time. Patient A remained free of significant infections on immunoglobulin replacement, prophylactic cotrimoxazole and fluconazole. Whilst on follow up, he presented aged 4 with severe macrocytic anemia (hemoglobin level 34 grams/L) requiring transfusion that was confirmed to be megaloblastic on bone marrow examination. Although stem cell transplant was considered in infancy, the lack of molecular diagnosis and clinical stability on prophylactic treatment persuaded the clinicians to delay this procedure indefinitely.

The younger sibling (patient B) was investigated at birth and found to have severe lymphopenia similar to his brother. He was given prophylactic cotrimoxazole and fluconazole. Immunoglobulin replacement was delayed in order to establish a better assessment of humoral immune function by vaccination. B was given the UK immunisation schedule primary course of inactivated vaccines between 2 and 5 months of age. Assessment of vaccine specific immunoglobulin response showed that he responded to protein (tetanus toxoid) but not conjugated polysaccharide (*Haemophilus influenzae* type B) vaccines (See table S3b in the online repository). Regular antibacterial (azithromycin) prophylaxis was added to his treatment regimen in view of poor humoral response to vaccines. Despite this, he was hospitalised with pneumococcal septic arthritis at 9 months of age after which immunoglobulin replacement was commenced. He remained susceptible to pyogenic bacterial infections, with further hospitalisations at 19 months (pneumonia), 22 months (peri-orbital cellulitis) and 24 months (pneumococcal bacteraemia). He also developed severe episodes of megaloblastic anemia during the course of his hospitalisation with septic arthritis at 9 months and pneumonia at 19 months of age.

Retrospective review of both patients' RBC indices revealed a persistent macrocytosis from young infancy (Fig 1). A detailed chronology of clinical manifestations is presented in the online repository (See case description in the online repository).

Immunological phenotype

Both patients have had severe persistent lymphopenia involving all lymphoid subsets (See tables S2a & S2b in the online repository). Both have had persistently low thymic output of T cells as measured by T-cell receptor excision circles (TRECs) (Fig 1). T lymphocyte subsets and T cell receptor (TCR) repertoire were normally distributed (data not shown). Lymphocyte proliferation to polyclonal (phytohaemagglutinin) and T lymphocyte specific (anti-CD3 & 28) stimuli have repeatedly been comparable to healthy controls (data not shown).

Both patients had low immunoglobulin levels involving all isotypes before immunoglobulin replacement therapy (Fig 1; Also see tables S3a & S3b in the online repository). Patient A did not complete his primary course of vaccines in infancy prior to immunoglobulin replacement therapy. Patient B showed defective response to conjugated polysaccharide vaccines in infancy (See table S3b in the online repository).

Subsequent to establishing the molecular diagnosis, we under took further in-vitro assays to assess T lymphocyte function. These demonstrated normal T lymphocyte activation, cytokine production and terminal differentiation. Taken together, this data suggested that although T lymphocyte numbers were low, T cell function was normal (See Figs S2a, 2b and 2c in the online repository). Additionally, assessments of antigen presenting cells including monocytes, myeloid and plasmacytoid dendritic cells were comparable to healthy controls (See Fig 1b in the online repository).

Response to folinic acid treatment

A presumed diagnosis of a defect in the folate metabolic pathway was made and both siblings were empirically treated with regular folinic acid supplement. As shown in figure 1, the mean corpuscular volume (MCV) normalised within weeks of supplementation. There have been no further episodes of anemia. In the first months of therapy there was a partial reconstitution of the lymphocyte compartment with absolute lymphocyte and all subsets returning to lower limits of normal for age (See tables S2a & S2b in the online repository). The CD4+ TREC count improved 10 fold in both patients (Fig 1). IgM (Fig 1) and IgA levels (See tables S3a & S3b in online repository) also improved to normal levels over months suggesting a reconstitution of the humoral compartment. Immunoglobulin supplements were discontinued and both patients have maintained normal levels of all isotypes during the subsequent four years of follow up (See table S3a & S3b in the online repository). They have both been re-immunised and have responded well to both protein and conjugate vaccines (See table S3a &

S3b in the online repository). Both patients have remained free of significant infections without prophylactic antibiotics or immunoglobulin replacement for 8 years since starting folinic acid therapy.

Exome Analysis

Suspecting a defect in folate metabolism without a single candidate gene, we undertook whole exome sequencing (WES) to analyze multiple gene variants (6). Interrogation of variants within genes involved in folic acid metabolism (GO:0046655(7)) for which the brothers were concordant identified a maternally inherited novel point mutation in exon 3, heterozygous T- to -C transition at c.152 position (c.152T>C; NM_005956.3), that would lead to a substitution of a conserved amino acid (p.Leu51Pro). This amino acid is situated within the methylenetetrahydrofolate dehydrogenase/cyclohydrogenase domain of C1-THF synthase and the amino acid substitution is predicted to adversely impact protein function. The base within the Leu-51 residue is well conserved evolutionarily, with a GERP++ score of 3.2(8). Leu-51 is located within a α-helix, with the adjacent Tyr-52 and the proximal Lys-56 involved in substrate binding within the dehydrogenase/cyclohydrolase active site (9). Proline residues are well documented to distort α-helices. The lack of an amide proton, coupled with the conformational rigidity of the cyclic residue canonically results in an approximately 30^0 bend in the helix (10) and the identified L51P mutation would be expected to distort this α-helix, reducing the affinity of the active site for the substrates.

In the previous report of C1-THF synthase deficiency, the heterozygous parents were reported to be asymptomatic (2). Structural variations (SVs) that are also important for Mendelian disease are not easily detected using an exome approach (11). Most exome studies conducted so far on specific diseases focus on single nucleotide variants, rather than SVs such as insertion/deletion variants (12). This is due in part to the fact that insertion/deletion bioinformatics analysis methodologies are still being refined. Read depth and split reads provide a clue to structural variants within exome data (13). Therefore, we extended our bioinformatic interrogation of the *MTHFD1* gene by manually examining sequencing depth coverage of the raw alignments in affected brothers compared to an unrelated individual concurrently sequenced. For exons with apparent reduced coverage, read depth was enumerated, normalized according to total aligned reads for the sample and assessed statistically (one tailed t-test) alongside 13 unrelated samples from the same sequencing batch, processed identically (Fig 2b). This process identified a paternally inherited deletion encompassing exon 13, in both brothers (Fig 2c).

Confirmation of mutation by Sanger sequencing

PCR amplification and Sanger sequencing using primers (Primers EX3F & EX3R; See table S1 in the online repository), confirmed that the novel point mutation in exon 3 was present in both patients and the mother but not the father (Fig 2d).

Identification by traditional sequencing of the breakpoints of exon deletions suspected on the basis of read depth coverage in the exome data can be arduous as the breakpoints are likely to be located in the intronic regions upstream and downstream of the identified exon which may span many thousands of base pairs (bps). However, we noted that in the read pile up of our patients, there were anomalous read pairs spanning over 2000 bps (Fig 2c). Primers were designed (Ex13LF & EX13LR; See table S1 in the online repository) to encompass this region. The predicted PCR product size in the reference template is 2350 bps (See Fig S4a in the online repository). PCR amplification of this region revealed an expected 2350 bps product in the mother but only a product of 600 base pairs in the patients, confirming a deletion involving exon 13 (Fig 2e). We were subsequently able to delineate the breakpoints accurately by Sanger sequencing of the above PCR products from the mother and patients (See Figs S3a & S3b in the online repository). We were also able to confirm the heterozygous state for deletion of exon 13 in the patients by allele specific PCR (See Fig S4a & S4b in the online repository). Further analysis revealed that the deletion boundaries were within homologous positions of flanking, parallel, AluS repeats (See Fig S5a & S5b in the online repository), previously observed as a pathogenic mutational mechanism in other genes, such as in *BRCA1* (14). For interested readers, further discussion is provided in the online repository.

Allelic expression at mRNA level

The deletion of exon 13 is predicted to introduce a premature stop codon resulting in a truncated protein of 422 amino acids. The nonsense mediated decay (NMD) pathway exists in eukaryotic cells to ensure fidelity of transcription and prevent translation of truncated proteins with potentially deleterious gain-of-function or dominant-negative activity (17). We hypothesised that the deletion of EX13 would target the mRNA from paternal allele (with a premature stop codon), for NMD. Allelic expression of the *MTHFD1* gene was undertaken using the point mutation in the exon 3 to analyse the relative expression of the maternal and paternal allele (18). *MTHFD1* cDNA was amplified using gene specific primers covering the point mutation in the EX3 (inherited from their

mother). As shown in the Fig 2f, the mRNA from the paternal allele was almost extinct confirming our hypothesis.

Discussion

Patients A and B carry compound heterozygous mutations consistent with autosomal recessive inheritance (Fig 2a), L51P inherited from their mother and deletion of exon 13 inherited from their father. *In silico* analysis of mutant L51P predicts an adverse impact on the function of the protein. A mutation in the vicinity (S49F) has recently been shown to be significantly less functional in biochemical studies (4). Allelic expression data is consistent with the deletion of exon 13 producing haploinsufficiency. The partial response to folinic acid therapy is consistent with a residual functioning enzyme as previously described (4).

MTHFD1 mutations cause highly variable clinical phenotypes with megaloblastic anemia being the only consistent feature (3, 4). This is likely the result of variable degree of residual enzyme function, but the limited number of patients currently reported makes it impossible to draw conclusions regarding genotype to phenotype correlation. Clinical manifestations described in smaller proportion of patients include severe immunodeficiency, haemolytic uremic syndrome (HUS), mild mental retardation, epilepsy and retinopathy. Severe immunodeficiency has been reported in 3 out 5 patients and was the most likely cause of mortality in two of the patients. Macrocytosis, lymphopenia involving all subsets and low TREC (Fig 1) were present from infancy in the patients reported here and may be a clue to the need to investigate folate metabolic pathways. *MTHFD1* deficiency should be considered in the aetiology of megaloblastic anemia where there are normal levels of vitamin B12 and folate; and in CID where there is macrocytosis..

We have characterized the immune function in our kindred that delineate the immune function in *MTHFD1* deficiency. The antigen presenting cells in the peripheral blood were present in normal numbers and responded to Toll Like Receptor (TLR) ligands in a comparable fashion to controls (data not shown). Both cell mediated and humoral immunity were defective in our patients. The clinical improvement in susceptibility to infections, partial reconstitution of cell numbers and improvement in both overall immunoglobulin levels and vaccine responses suggest that the immunodeficiency cause by this condition can be reversed to a large extent with folinic acid treatment.

The major limitation of exome sequencing is the inability to comprehensively represent genomic structural variations (SVs) such as deletions, inversions or duplications (11). Many groups have designed algorithms that use a read depth or read pair-based approach for predicting structural variation. However, these approaches are not very efficient at identifying SVs with exome data due to

the discontinuous nature of the data, with only ~ 1% of the genome having significant read coverage (19). Our approach was successful in identifying the exon 13 deletion due to strong clinical suspicion. While it may not be possible to detect all forms of structural variations, we have demonstrated the possibility of analysing specific genes using read depth, split reads and read pairs to provide clues to structural variants. Where improved detection of structural variants are required, whole-genome sequencing (WGS) should be used.

The importance of establishing a definitive molecular diagnosis in children with primary immunodeficiency cannot be overemphasized. Both patients were considered to have SCID and were on the bone marrow transplant list for the first few years of life. Knowledge of the specific molecular diagnosis has led to the identification of a precision treatment in the form of life-long folinic acid supplementation. Other prophylactic therapies have been able to be discontinued. The responsiveness of this disorder to folinic acid supplementation emphasizes the importance of precision diagnostics in the diagnosis of primary immunodeficiency prior to the consideration of stem cell transplantation, and to stratify appropriate treatment modalities to reduce risk and improve outcomes. Clinical exome sequencing, even in single families, is a powerful adjunct to the investigation of metabolic pathways that may lead to distinctive immunodeficiency disorders.

Acknowledgements

YG and APW were supported by Cancer Research UK and the Experimental Cancer Medicine Centre, Southampton. KR and SNF received support from the Southampton NIHR Wellcome Trust Clinical Research Facility.

Disclaimer

The authors declare no competing financial interests.

References

1. Whitehead VM. Acquired and inherited disorders of cobalamin and folate in children. British journal of haematology. 2006;134(2):125-36.

2. Watkins D, Schwartzentruber JA, Ganesh J, Orange JS, Kaplan BS, Nunez LD, et al. Novel inborn error of folate metabolism: identification by exome capture and sequencing of mutations in the MTHFD1 gene in a single proband. Journal of medical genetics. 2011;48(9):590-2.

3. Keller MD, Ganesh J, Heltzer M, Paessler M, Bergqvist AG, Baluarte HJ, et al. Severe combined immunodeficiency resulting from mutations in MTHFD1. Pediatrics. 2013;131(2):e629-34.

4. Burda P, Kuster A, Hjalmarson O, Suormala T, Burer C, Lutz S, et al. Characterization and review of MTHFD1 deficiency: four new patients, cellular delineation and response to folic and folinic acid treatment. Journal of inherited metabolic disease. 2015.

5. Pengelly RJ, Upstill-Goddard R, Arias L, Martinez J, Gibson J, Knut M, et al. Resolving clinical diagnoses for syndromic cleft lip and/or palate phenotypes using whole-exome sequencing. Clinical genetics. 2014.

6. Harding KE, Robertson NP. Applications of next-generation whole exome sequencing. Journal of neurology. 2014;261(6):1244-6.

7. The Gene Ontology. Available from: http://www.geneontology.org/.

8. Davydov EV, Goode DL, Sirota M, Cooper GM, Sidow A, Batzoglou S. Identifying a high fraction of the human genome to be under selective constraint using GERP++. PLoS computational biology. 2010;6(12):e1001025.

9. Allaire M, Li Y, MacKenzie RE, Cygler M. The 3-D structure of a folate-dependent dehydrogenase/cyclohydrolase bifunctional enzyme at 1.5 A resolution. Structure. 1998;6(2):173-82.

10. Rey J, Deville J, Chabbert M. Structural determinants stabilizing helical distortions related to proline. Journal of structural biology. 2010;171(3):266-76.

11. Biesecker LG, Shianna KV, Mullikin JC. Exome sequencing: the expert view. Genome biology. 2011;12(9):128.

12. Lescai F, Bonfiglio S, Bacchelli C, Chanudet E, Waters A, Sisodiya SM, et al. Characterisation and validation of insertions and deletions in 173 patient exomes. PloS one. 2012;7(12):e51292.

13. Zhao M, Wang Q, Wang Q, Jia P, Zhao Z. Computational tools for copy number variation (CNV) detection using next-generation sequencing data: features and perspectives. BMC bioinformatics. 2013;14 Suppl 11:S1.

14. Tancredi M, Sensi E, Cipollini G, Aretini P, Lombardi G, Di Cristofano C, et al. Haplotype analysis of BRCA1 gene reveals a new gene rearrangement: characterization of a 19.9 KBP deletion. European journal of human genetics : EJHG. 2004;12(9):775-7.

15. Chang YF, Imam JS, Wilkinson MF. The nonsense-mediated decay RNA surveillance pathway. Annual review of biochemistry. 2007;76:51-74.

16. Hsu AP, Johnson KD, Falcone EL, Sanalkumar R, Sanchez L, Hickstein DD, et al. GATA2 haploinsufficiency caused by mutations in a conserved intronic element leads to MonoMAC syndrome. Blood. 2013;121(19):3830-7, S1-7.

17. Biesecker LG. Editorial comment on "Whole exome sequencing identifies compound heterozygous mutations in WDR62 in siblings with recurrent polymicrogyria". American journal of medical genetics Part A. 2011;155A(9):2069-70.

Figure legends

Fig 1: Response to folinic acid treatment in patients A and B. Both brothers received parenteral folinic acid treatment for 2 weeks at the time point indicated by the first arrow and regular enteral supplement from the time point indicated by the second arrow.

Fig 2. Molecular diagnosis. Where not shown, patient A's results were representative of patient B. 2a: Pedigree showing affectation with disease. Black fill –affected, '+' – whole-exome sequenced. 2b: Depth of coverage for exons in MTHFD1 in 13 control samples and the three cases, indicating an exon 13 deletion in the three whole-exome sequenced family members (p=0.00019 for depth between cases and controls). 2c: Summary of evidence for exon 13 deletion in NGS data. Chromosomal location is indicated on karyogram, expanded below into coordinates. Read depth in representative case (Patient A) is shown, alongside a representative unrelated control sample from the same batch. It can be seen that read depth in our case is approximately half that of the control. Furthermore, in the case read pileup an anomalous excessive read pair span can be seen (highlighted in red). Read pairs are derived

from opposing ends of a single contiguous fragment of DNA. Presuming that the DNA fragment sequenced falls within the expected length range (representative reads pairs can be seen in pileup in grey), and that the reads are aligned to the reference genome correctly, the extended apparent read pair span would indicate a deletion within the encompassed genomic region. As such, PCR primers were designed flanking the anomalous read pair. Upon Sanger sequencing of the resultant amplicon, a 1,745 bps deletion was observed. 2d: Sanger sequencing of MTHFD1 exon3 showing c.T152C:p.L51P which is present both brothers and mother but not the father. 2e: Sequencing of MTHFD1 gene yielded the expected PCR product of 2350 bps in the mother (lane 5) and a PCR product of around 600 bps in the patients and father (lane 2-4). 2f: Sanger sequencing of gDNA and cDNA of the patient A revealed the presence of the 2 alleles at the genomic level but only expression of the mother's allele at the cDNA level.

TITLE PAGE

Title

Precision molecular diagnosis defines specific therapy in combined immunodeficiency with megaloblastic anaemia secondary to *MTHFD1* deficiency.

Concise title

Combined immunodeficiency caused by *MTHFD1* deficiency

Authors

Kesava A. Ramakrishnan MD[1*], Reuben J. Pengelly PhD[3*], Yifang Gao PhD[2], Mary Morgan FRCPath[4], Sanjay V. Patel MD[4], Graham Davies MD[5], Sarah Ennis PhD[3], Saul N. Faust MD, PhD[1,4], Anthony P. Williams MD, PhD[2,6]

Affiliations

[1]Academic Unit of Clinical and Experimental Sciences, Faculty of Medicine and Institute for Life Sciences, University of Southampton and NIHR Biomedical Respiratory Unit, University Hospital Southampton NHS Foundation Trust, Southampton, UK.

[2]Academic Unit of Cancer Sciences, Faculty of Medicine and Institute for Life Sciences, University of Southampton, and CRUK NIHR Experimental Cancer Medicine Centre

[3]Academic Unit of Human Development and Health, Human Genetics and Genomic Medicine, Faculty of Medicine, University of Southampton, Southampton, UK.

[4]Southampton NIHR Wellcome Trust Clinical Research Facility and Department of Paediatric Medicine, University Hospital Southampton NHS Foundation Trust, Southampton, UK.

[5]Department of Paediatric Immunology, Great Ormond Street Hospital for Children NHS Foundation Trust, London, UK.

[6]Department of Allergy, Asthma and Clinical Immunology, University Hospital Southampton NHS Foundation Trust, Southampton, UK.

*** These authors contributed equally.**

Contact for Correspondence

Professor Saul Faust

Southampton NIHR Wellcome Trust Clinical Research Facility, Mailpoint 218, University Hospital Southampton NHS Foundation Trust, Southampton, SO16 6YD, UK.

Tel: 023 8120 4939

Fax: 023 8120 5023

E Mail: S.Faust@soton.ac.uk

Word Count

Abstract - 143

Text – 2849

Number of figures – 2

Number of references - 17

Key Words

Megaloblastic anemia

C-1-tetrahydrofolate synthase, cytoplasmic (C1-THF synthase)

Folinic acid

Combined Immunodeficiency

Lymphopenia

Abbreviations

MTHFD1 – Methylenetetrahydrofolate dehydrogenase 1

SCID – Severe combined immunodeficiency

PCP - *Pneumocystic jirovecii* pneumonia

TRECs - T-cell receptor excision circles

PBMCs - Peripheral blood mononuclear cells

TH1 – T helper 1

TH17 – T helper 17

cDNA – Complementary DNA

PCR – Polymerase chain reaction

TCR – T cell receptor

CD_{XX} – Cluster of differentiation molecule

Anti-CD_{XX} – Monoclonal antibody to CD_{XX}

IFNγ – Interferon γ

IL-17 – Interleukin 17

WES – Whole exome sequencing

WGS – Whole genome sequencing

Highlights

1. What is already known about this topic? Recessively inherited MTHFD1 deficiency has previously been described to present with a severe combined immunodeficiency
2. What does this article add to our knowledge? Exome sequencing demonstrated *MTHFD1* deficiency as a novel cause of a combined immunodeficiency and folinic acid was established as precision therapy to reverse the clinical and laboratory phenotype.
3. How does this study impact current management guidelines? Early use of new molecular diagnostic techniques can personalise treatment in managing unexplained immunodeficiencies and in some cases prevent the need for bone marrow transplantation.

Abstract

Background: Methylenetetrahydrofolate dehydrogenase *(MTHFD1)* deficiency has recently been reported to cause a folate responsive syndrome displaying a phenotype that includes megaloblastic anemia and severe combined immunodeficiency (SCID).

Objective: To describe our investigative approach to the molecular diagnosis and evaluation of immune dysfunction in a family with *MTHFD1* deficiency.

Methods: Exome sequencing and analysis of variants in genes involved in the folate metabolic pathway in a family with two affected siblings. Routine laboratory and research data were analyzed to gain an in depth understanding of innate, humoral and cell mediated immune function before and after folinic acid supplementation.

Results: Interrogation of exome data for concordant variants between the siblings in the genes involved in folate metabolic pathway identified a heterozygous mutation in exon 3 of the MTHFD1 gene that was shared with their mother.

In view of highly suggestive phenotype, we extended our bioinformatics interrogation for structural variants in the MTHFD1 gene by manual evaluation of the exome data for sequence depth coverage of all the exons. A deletion involving exon 13 that was shared with their father was identified.

Routine laboratory data showed lymphopenia involving all subsets and poor response to vaccines. In-vitro analysis of dendritic cell and lymphocyte function were comparable to healthy volunteers. Treatment with folinic acid led to immune reconstitution enabling discontinuation of all prophylactic therapies.

Conclusion: Exome sequencing demonstrated *MTHFD1* deficiency as a novel cause of a combined immunodeficiency. Folinic acid was established as precision therapy to reverse the clinical and laboratory phenotype of this primary immunodeficiency.

Introduction

Derivatives of folic acid play a critical role in cellular one carbon metabolism, acting as donors and recipients of one-carbon units involved in synthesis and breakdown of amino acids as well as in the synthesis of thymidine and purines (1). C-1-tetrahydrofolate synthase (C1-THF synthase) is a cytoplasmic tri-functional enzyme essential for processing single carbon folate derivatives, encoded by the gene methylenetetrahydrofolate dehydrogenase *(MTHFD1)*. Mutations in *MTHFD1* have previously been reported to cause a syndrome displaying megaloblastic anemia, severe combined immunodeficiency (SCID), mild mental retardation and treatment-refractory epilepsy that was responsive to metabolic supplementation (2, 3). Four further case reports (4), two whom died of overwhelming sepsis have extended the phenotype to include atypical hemolytic uremic syndrome, microangiopathy and retinopathy. We present the long term follow up data of a family with two siblings who carry novel compound heterozygous mutations in the *MTHFD1* gene. Specifically, we have characterized the immune function in more detail and documented the response in immune function to folinic acid supplementation.

Methods

Subjects: Two brothers born to a mother of Southeast Asian and father of Caucasian origin managed in our specialist immunology service for more than a decade. Consent for research investigations was obtained (NHS Research Ethics 09/H502/4).

Exome Sequencing: Exome enrichment was performed using the SureSelect Human All Exon V4.0 kit (Agilent), prior to sequencing on the Illumina HiSeq 2000 system. Following sequencing, data processing was performed as previously described (5).

PCR amplification: PCR was performed according to manufacturer instruction using a Phusion high-fidelity PCR kit from Thermo Scientific. PCR conditions and primer sequences used for amplification exons 3 and 13 are summarized in table S1 in the online repository.

RNA amplification: RNA was extracted from lithium heparin anti-coagulated whole blood using QIAamp RNA Blood Mini Kit (Qiagen Uk). 200 ng of total RNA was reverse transcribed and cDNA amplified using MTHFD1 gene specific primers (cDNAF and cDNAR) as per manufacturer instructions using SuperScript™ III One-Step RT-PCR System (Life technologies).

Flow cytometry: A two step staining process for surface and intracellular antigens was performed according to manufacturer instructions using BD fix-perm kit. Flow cytometry data were acquired on a BD FACS canto II. At least 200,000 events were collected for lymphocyte assays and 500,000 for the dendritic cell assays. Data were analyzed using FACS Diva software and gating strategy is illustrated in the supplementary figures 1 & 2.

Results

Clinical manifestations

The elder sibling (patient A) presented at 4 months of age with clinical and radiological features consistent with *Pneumocystic jirovecii* pneumonia (PCP). SCID was diagnosed on the basis of susceptibility to PCP and severe lymphopenia involving all lymphoid subsets. Subsequent investigations found no mutations in the genes known to cause SCID at that time. Patient A remained free of significant infections on immunoglobulin replacement, prophylactic cotrimoxazole and fluconazole. Whilst on follow up, he presented aged 4 with severe macrocytic anemia (hemoglobin level 34 grams/L) requiring transfusion that was confirmed to be megaloblastic on bone marrow examination. Although stem cell transplant was considered in infancy, the lack of molecular diagnosis and clinical stability on prophylactic treatment persuaded the clinicians to delay this procedure indefinitely.

The younger sibling (patient B) was investigated at birth and found to have severe lymphopenia similar to his brother. He was given prophylactic cotrimoxazole and fluconazole. Immunoglobulin replacement was delayed in order to establish a better assessment of humoral immune function by vaccination. B was given the UK immunisation schedule primary course of inactivated vaccines between 2 and 5 months of age. Assessment of vaccine specific immunoglobulin response showed that he responded to protein (tetanus toxoid) but not conjugated polysaccharide (*Haemophilus influenzae* type B) vaccines (See table S3b in the online repository). Regular antibacterial (azithromycin) prophylaxis was added to his treatment regimen in view of poor humoral response to vaccines. Despite this, he was hospitalised with pneumococcal septic arthritis at 9 months of age after which immunoglobulin replacement was commenced. He remained susceptible to pyogenic bacterial infections, with further hospitalisations at 19 months (pneumonia), 22 months (peri-orbital cellulitis) and 24 months (pneumococcal bacteraemia). He also developed severe episodes of megaloblastic anemia during the course of his hospitalisation with septic arthritis at 9 months and pneumonia at 19 months of age.

Retrospective review of both patients' RBC indices revealed a persistent macrocytosis from young infancy (Fig 1). A detailed chronology of clinical manifestations is presented in the online repository (See case description in the online repository).

Immunological phenotype

Both patients have had severe persistent lymphopenia involving all lymphoid subsets (See tables S2a & S2b in the online repository). Both have had persistently low thymic output of T cells as measured by T-cell receptor excision circles (TRECs) (Fig 1). T lymphocyte subsets and T cell receptor (TCR) repertoire were normally distributed (data not shown). Lymphocyte proliferation to polyclonal (phytohaemagglutinin) and T lymphocyte specific (anti-CD3 & 28) stimuli have repeatedly been comparable to healthy controls (data not shown).

Both patients had low immunoglobulin levels involving all isotypes before immunoglobulin replacement therapy (Fig 1; Also see tables S3a & S3b in the online repository). Patient A did not complete his primary course of vaccines in infancy prior to immunoglobulin replacement therapy. Patient B showed defective response to conjugated polysaccharide vaccines in infancy (See table S3b in the online repository).

Subsequent to establishing the molecular diagnosis, we under took further in-vitro assays to assess T lymphocyte function. These demonstrated normal T lymphocyte activation, cytokine production and terminal differentiation. Taken together, this data suggested that although T lymphocyte numbers were low, T cell function was normal (See Figs S2a, 2b and 2c in the online repository). Additionally, assessments of antigen presenting cells including monocytes, myeloid and plasmacytoid dendritic cells were comparable to healthy controls (See Fig 1b in the online repository).

Response to folinic acid treatment

A presumed diagnosis of a defect in the folate metabolic pathway was made and both siblings were empirically treated with regular folinic acid supplement. As shown in figure 1, the mean corpuscular volume (MCV) normalised within weeks of supplementation. There have been no further episodes of anemia. In the first months of therapy there was a partial reconstitution of the lymphocyte compartment with absolute lymphocyte and all subsets returning to lower limits of normal for age (See tables S2a & S2b in the online repository). The CD4+ TREC count improved 10 fold in both patients (Fig 1). IgM (Fig 1) and IgA levels (See tables S3a & S3b in online repository) also improved to normal levels over months suggesting a reconstitution of the humoral compartment. Immunoglobulin supplements were discontinued and both patients have maintained normal levels of all isotypes during the subsequent four years of follow up (See table S3a & S3b in the online repository). They have both been re-immunised and have responded well to both protein and conjugate vaccines (See table S3a &

S3b in the online repository). Both patients have remained free of significant infections without prophylactic antibiotics or immunoglobulin replacement for 8 years since starting folinic acid therapy.

Exome Analysis

Suspecting a defect in folate metabolism without a single candidate gene, we undertook whole exome sequencing (WES) to analyze multiple gene variants (6). Interrogation of variants within genes involved in folic acid metabolism (GO:0046655(7)) for which the brothers were concordant identified a maternally inherited novel point mutation in exon 3, heterozygous T- to -C transition at c.152 position (c.152T>C; NM_005956.3), that would lead to a substitution of a conserved amino acid (p.Leu51Pro). This amino acid is situated within the methylenetetrahydrofolate dehydrogenase/cyclohydrogenase domain of C1-THF synthase and the amino acid substitution is predicted to adversely impact protein function. The base within the Leu-51 residue is well conserved evolutionarily, with a GERP++ score of 3.2(8). Leu-51 is located within a α-helix, with the adjacent Tyr-52 and the proximal Lys-56 involved in substrate binding within the dehydrogenase/cyclohydrolase active site (9). Proline residues are well documented to distort α-helices. The lack of an amide proton, coupled with the conformational rigidity of the cyclic residue canonically results in an approximately 30^0 bend in the helix (10) and the identified L51P mutation would be expected to distort this α-helix, reducing the affinity of the active site for the substrates.

In the previous report of C1-THF synthase deficiency, the heterozygous parents were reported to be asymptomatic (2). Structural variations (SVs) that are also important for Mendelian disease are not easily detected using an exome approach (11). Most exome studies conducted so far on specific diseases focus on single nucleotide variants, rather than SVs such as insertion/deletion variants (12). This is due in part to the fact that insertion/deletion bioinformatics analysis methodologies are still being refined. Read depth and split reads provide a clue to structural variants within exome data (13). Therefore, we extended our bioinformatic interrogation of the *MTHFD1* gene by manually examining sequencing depth coverage of the raw alignments in affected brothers compared to an unrelated individual concurrently sequenced. For exons with apparent reduced coverage, read depth was enumerated, normalized according to total aligned reads for the sample and assessed statistically (one tailed t-test) alongside 13 unrelated samples from the same sequencing batch, processed identically (Fig 2b). This process identified a paternally inherited deletion encompassing exon 13, in both brothers (Fig 2c).

Confirmation of mutation by Sanger sequencing

PCR amplification and Sanger sequencing using primers (Primers EX3F & EX3R; See table S1 in the online repository), confirmed that the novel point mutation in exon 3 was present in both patients and the mother but not the father (Fig 2d).

Identification by traditional sequencing of the breakpoints of exon deletions suspected on the basis of read depth coverage in the exome data can be arduous as the breakpoints are likely to be located in the intronic regions upstream and downstream of the identified exon which may span many thousands of base pairs (bps). However, we noted that in the read pile up of our patients, there were anomalous read pairs spanning over 2000 bps (Fig 2c). Primers were designed (Ex13LF & EX13LR; See table S1 in the online repository) to encompass this region. The predicted PCR product size in the reference template is 2350 bps (See Fig S4a in the online repository). PCR amplification of this region revealed an expected 2350 bps product in the mother but only a product of 600 base pairs in the patients, confirming a deletion involving exon 13 (Fig 2e). We were subsequently able to delineate the breakpoints accurately by Sanger sequencing of the above PCR products from the mother and patients (See Figs S3a & S3b in the online repository). We were also able to confirm the heterozygous state for deletion of exon 13 in the patients by allele specific PCR (See Fig S4a & S4b in the online repository). Further analysis revealed that the deletion boundaries were within homologous positions of flanking, parallel, AluS repeats (See Fig S5a & S5b in the online repository), previously observed as a pathogenic mutational mechanism in other genes, such as in *BRCA1* (14). For interested readers, further discussion is provided in the online repository.

Allelic expression at mRNA level

The deletion of exon 13 is predicted to introduce a premature stop codon resulting in a truncated protein of 422 amino acids. The nonsense mediated decay (NMD) pathway exists in eukaryotic cells to ensure fidelity of transcription and prevent translation of truncated proteins with potentially deleterious gain-of-function or dominant-negative activity (17). We hypothesised that the deletion of EX13 would target the mRNA from paternal allele (with a premature stop codon), for NMD. Allelic expression of the *MTHFD1* gene was undertaken using the point mutation in the exon 3 to analyse the relative expression of the maternal and paternal allele (18). *MTHFD1* cDNA was amplified using gene specific primers covering the point mutation in the EX3 (inherited from their

mother). As shown in the Fig 2f, the mRNA from the paternal allele was almost extinct confirming our hypothesis.

Discussion

Patients A and B carry compound heterozygous mutations consistent with autosomal recessive inheritance (Fig 2a), L51P inherited from their mother and deletion of exon 13 inherited from their father. *In silico* analysis of mutant L51P predicts an adverse impact on the function of the protein. A mutation in the vicinity (S49F) has recently been shown to be significantly less functional in biochemical studies (4). Allelic expression data is consistent with the deletion of exon 13 producing haploinsufficiency. The partial response to folinic acid therapy is consistent with a residual functioning enzyme as previously described (4).

MTHFD1 mutations cause highly variable clinical phenotypes with megaloblastic anemia being the only consistent feature (3, 4). This is likely the result of variable degree of residual enzyme function, but the limited number of patients currently reported makes it impossible to draw conclusions regarding genotype to phenotype correlation. Clinical manifestations described in smaller proportion of patients include severe immunodeficiency, haemolytic uremic syndrome (HUS), mild mental retardation, epilepsy and retinopathy. Severe immunodeficiency has been reported in 3 out 5 patients and was the most likely cause of mortality in two of the patients. Macrocytosis, lymphopenia involving all subsets and low TREC (Fig 1) were present from infancy in the patients reported here and may be a clue to the need to investigate folate metabolic pathways. *MTHFD1* deficiency should be considered in the aetiology of megaloblastic anemia where there are normal levels of vitamin B12 and folate; and in CID where there is macrocytosis..

We have characterized the immune function in our kindred that delineate the immune function in *MTHFD1* deficiency. The antigen presenting cells in the peripheral blood were present in normal numbers and responded to Toll Like Receptor (TLR) ligands in a comparable fashion to controls (data not shown). Both cell mediated and humoral immunity were defective in our patients. The clinical improvement in susceptibility to infections, partial reconstitution of cell numbers and improvement in both overall immunoglobulin levels and vaccine responses suggest that the immunodeficiency cause by this condition can be reversed to a large extent with folinic acid treatment.

The major limitation of exome sequencing is the inability to comprehensively represent genomic structural variations (SVs) such as deletions, inversions or duplications (11). Many groups have designed algorithms that use a read depth or read pair-based approach for predicting structural variation. However, these approaches are not very efficient at identifying SVs with exome data due to

the discontinuous nature of the data, with only ~ 1% of the genome having significant read coverage (19). Our approach was successful in identifying the exon 13 deletion due to strong clinical suspicion. While it may not be possible to detect all forms of structural variations, we have demonstrated the possibility of analysing specific genes using read depth, split reads and read pairs to provide clues to structural variants. Where improved detection of structural variants are required, whole-genome sequencing (WGS) should be used.

The importance of establishing a definitive molecular diagnosis in children with primary immunodeficiency cannot be overemphasized. Both patients were considered to have SCID and were on the bone marrow transplant list for the first few years of life. Knowledge of the specific molecular diagnosis has led to the identification of a precision treatment in the form of life-long folinic acid supplementation. Other prophylactic therapies have been able to be discontinued. The responsiveness of this disorder to folinic acid supplementation emphasizes the importance of precision diagnostics in the diagnosis of primary immunodeficiency prior to the consideration of stem cell transplantation, and to stratify appropriate treatment modalities to reduce risk and improve outcomes. Clinical exome sequencing, even in single families, is a powerful adjunct to the investigation of metabolic pathways that may lead to distinctive immunodeficiency disorders.

Acknowledgements

YG and APW were supported by Cancer Research UK and the Experimental Cancer Medicine Centre, Southampton. KR and SNF received support from the Southampton NIHR Wellcome Trust Clinical Research Facility.

Disclaimer

The authors declare no competing financial interests.

References

1. Whitehead VM. Acquired and inherited disorders of cobalamin and folate in children. British journal of haematology. 2006;134(2):125-36.

2. Watkins D, Schwartzentruber JA, Ganesh J, Orange JS, Kaplan BS, Nunez LD, et al. Novel inborn error of folate metabolism: identification by exome capture and sequencing of mutations in the MTHFD1 gene in a single proband. Journal of medical genetics. 2011;48(9):590-2.

3. Keller MD, Ganesh J, Heltzer M, Paessler M, Bergqvist AG, Baluarte HJ, et al. Severe combined immunodeficiency resulting from mutations in MTHFD1. Pediatrics. 2013;131(2):e629-34.

4. Burda P, Kuster A, Hjalmarson O, Suormala T, Burer C, Lutz S, et al. Characterization and review of MTHFD1 deficiency: four new patients, cellular delineation and response to folic and folinic acid treatment. Journal of inherited metabolic disease. 2015.

5. Pengelly RJ, Upstill-Goddard R, Arias L, Martinez J, Gibson J, Knut M, et al. Resolving clinical diagnoses for syndromic cleft lip and/or palate phenotypes using whole-exome sequencing. Clinical genetics. 2014.

6. Harding KE, Robertson NP. Applications of next-generation whole exome sequencing. Journal of neurology. 2014;261(6):1244-6.

7. The Gene Ontology. Available from: http://www.geneontology.org/.

8. Davydov EV, Goode DL, Sirota M, Cooper GM, Sidow A, Batzoglou S. Identifying a high fraction of the human genome to be under selective constraint using GERP++. PLoS computational biology. 2010;6(12):e1001025.

9. Allaire M, Li Y, MacKenzie RE, Cygler M. The 3-D structure of a folate-dependent dehydrogenase/cyclohydrolase bifunctional enzyme at 1.5 A resolution. Structure. 1998;6(2):173-82.

10. Rey J, Deville J, Chabbert M. Structural determinants stabilizing helical distortions related to proline. Journal of structural biology. 2010;171(3):266-76.

11. Biesecker LG, Shianna KV, Mullikin JC. Exome sequencing: the expert view. Genome biology. 2011;12(9):128.

12. Lescai F, Bonfiglio S, Bacchelli C, Chanudet E, Waters A, Sisodiya SM, et al. Characterisation and validation of insertions and deletions in 173 patient exomes. PloS one. 2012;7(12):e51292.

13. Zhao M, Wang Q, Wang Q, Jia P, Zhao Z. Computational tools for copy number variation (CNV) detection using next-generation sequencing data: features and perspectives. BMC bioinformatics. 2013;14 Suppl 11:S1.

14. Tancredi M, Sensi E, Cipollini G, Aretini P, Lombardi G, Di Cristofano C, et al. Haplotype analysis of BRCA1 gene reveals a new gene rearrangement: characterization of a 19.9 KBP deletion. European journal of human genetics : EJHG. 2004;12(9):775-7.

15. Chang YF, Imam JS, Wilkinson MF. The nonsense-mediated decay RNA surveillance pathway. Annual review of biochemistry. 2007;76:51-74.

16. Hsu AP, Johnson KD, Falcone EL, Sanalkumar R, Sanchez L, Hickstein DD, et al. GATA2 haploinsufficiency caused by mutations in a conserved intronic element leads to MonoMAC syndrome. Blood. 2013;121(19):3830-7, S1-7.

17. Biesecker LG. Editorial comment on "Whole exome sequencing identifies compound heterozygous mutations in WDR62 in siblings with recurrent polymicrogyria". American journal of medical genetics Part A. 2011;155A(9):2069-70.

Figure legends

Fig 1: Response to folinic acid treatment in patients A and B. Both brothers received parenteral folinic acid treatment for 2 weeks at the time point indicated by the first arrow and regular enteral supplement from the time point indicated by the second arrow.

Fig 2. Molecular diagnosis. Where not shown, patient A's results were representative of patient B. 2a: Pedigree showing affectation with disease. Black fill –affected, '+' – whole-exome sequenced. 2b: Depth of coverage for exons in MTHFD1 in 13 control samples and the three cases, indicating an exon 13 deletion in the three whole-exome sequenced family members (p=0.00019 for depth between cases and controls). 2c: Summary of evidence for exon 13 deletion in NGS data. Chromosomal location is indicated on karyogram, expanded below into coordinates. Read depth in representative case (Patient A) is shown, alongside a representative unrelated control sample from the same batch. It can be seen that read depth in our case is approximately half that of the control. Furthermore, in the case read pileup an anomalous excessive read pair span can be seen (highlighted in red). Read pairs are derived

from opposing ends of a single contiguous fragment of DNA. Presuming that the DNA fragment sequenced falls within the expected length range (representative reads pairs can be seen in pileup in grey), and that the reads are aligned to the reference genome correctly, the extended apparent read pair span would indicate a deletion within the encompassed genomic region. As such, PCR primers were designed flanking the anomalous read pair. Upon Sanger sequencing of the resultant amplicon, a 1,745 bps deletion was observed. 2d: Sanger sequencing of MTHFD1 exon3 showing c.T152C:p.L51P which is present both brothers and mother but not the father. 2e: Sequencing of MTHFD1 gene yielded the expected PCR product of 2350 bps in the mother (lane 5) and a PCR product of around 600 bps in the patients and father (lane 2-4). 2f: Sanger sequencing of gDNA and cDNA of the patient A revealed the presence of the 2 alleles at the genomic level but only expression of the mother's allele at the cDNA level.

ON LINE REPOSITORY MATERIAL:

Precision molecular diagnosis defines specific therapy in combined immunodeficiency with megaloblastic anaemia secondary to *MTHFD1* deficiency.

Index:

Case Description

The first child (patient A) presented at 4 months of age with a two - week history of breathlessness, poor feeding and weight loss. His chest X-ray was consistent with *Pneumocystis Jirovecii* pneumonia (PCP), which was confirmed on bronchoalveolar lavage. He was suspected to have severe combined immunodeficiency (SCID) on the basis of lymphopenia ($0.9x\ 10^9$/L), which involved all the lymphoid subsets. HIV tests were negative and extensive investigations excluded all known SCID gene defects. Although he had T lymphopenia, he had normal distribution of subsets, T-cell- receptor (TCR) repertoire and his proliferation to phytohaemagglutinin (PHA) was comparable to control. A diagnosis of undefined SCID was made and he was listed for a hematopoietic stem cell transplant (HSCT). After his recovery from PCP, he was discharged home on cotrimoxazole, fluconazole and subcutaneous immunoglobulin (SCIG), awaiting a matched donor. Patient A was born to a South Asian mother and Caucasian father at 36+6 weeks gestation. His elder sister was reported to be healthy and there was no significant family history of immunodeficiency or metabolic disorders. The mother was known to carry hepatitis B virus. At 2 months of age, he was found to be anemic despite apparently thriving normally. Investigation for hemolytic anaemia was negative and symptoms resolved with folate and iron supplements for 2 weeks. HSCT was postponed despite finding a well-matched unrelated donor, as he remained clinically well with an improving immunological picture. Although he did not suffer significant infections, he remained lymphopenic and the evolving hypogammaglobulinemia led to reconsideration of HSCT. In the interim, his mother became pregnant and HSCT was postponed in view of his progress, the lack of ongoing opportunistic infections and a potential for getting a better donor match when the sibling was born.

His brother (patient B) was born when his elder sibling was 18 months old and displayed similar lymphopenia to his elder patient. He was started on fluconazole and cotrimoxazole prophylaxis soon after diagnosis, but IVIG was withheld to try to establish better immunological assessment. He was immunized with inactivated vaccines between 2 and 5 months according to the UK infant immunization programme. His immunoglobulin levels dropped below normal limits by the age of 6 months and although he responded to tetanus he did not respond to conjugated HiB vaccine (table s3b) and he was therefore started on azithromycin prophylaxis at 6 months of age. Subsequently he presented at 9 months of age with septic arthritis of his left hip. Blood culture and joint aspiration pus identified *Streptococcus pneumoniae*. While patient B was still hospitalized, patient A presented with a 1 week history of pallor and was found to be severely anemic (Hb 34 gms/L). Bone marrow examination

showed a marked megaloblastic picture. RBC folate and Vitamin B12 levels were within normal limits, therefore cotrimoxazole was considered to be a potential cause. Patient B also became anemic during the course of his septic arthritis treatment (Hb 6.4 gms/dl). Bone marrow examination performed at this time showed a megaloblastic picture and cotrimoxazole was discontinued. Both boys were treated with a two-week course of parenteral vitamin B12 & calcium folinate. Patient A was started on pentamidine nebulizers for PCP prophylaxis. Due to parental concern regarding medicalization and therapy safety, patient B was not given any PCP prophylaxis. Patient B was started on subcutaneous immunoglobulin therapy at 10 months of age. Despite this, patient B suffered further pyogenic infections that included pneumonia (organism not isolated) at 19 months, peri-orbital cellulitis at 22 months and pneumococcal bacteremia at 24 months. The infection at 19 months of age was accompanied by a further episode of megaloblastic anemia.

Immunological evaluations revealed that both patients were lymphopenic for all subsets throughout their follow up (Table S2a & S2b). Both patients had low IgM levels whilst on immunoglobulin replacement therapy suggestive of antibody deficiency. Patient A was not immunized in infancy whilst patient B was vaccinated with inactive vaccines and showed adequate tetanus titers but did not develop protective HiB titers (Table S3b).

T cell subsets expressed memory markers in a pattern similar to healthy controls (data shown in main article). T cell subsets expressed activation marker CD69 in response to TCR specific stimuli (data shown in main article). T helper subset enumeration showed comparable numbers of TH1 & TH17 development (data shown in main article). Both siblings continued to have normal T cell proliferation, but their T cell receptor excision circle (TREC) counts remained low suggestive of low thymic output. Following the initiation of calcium folinate supplementation both patients have remained free of infections and have mounted protective vaccine responses following the cessation of immunoglobulin replacement therapy (Table S3a & S3b). Both patients are in regular schools with no disabilities identified. Both had normal MRI brain and plasma/CSF folate studies before regular folinic acid supplements were started. Following their successful treatment and identification of the molecular cause the family have been informed that HSCT is no longer a therapeutic consideration.

Immunological experiments

Methods:

Cell culture: Lithium heparin anticoagulated blood samples were obtained from the patients and experiments were set up within 4 hours of sampling. Whole blood was diluted 1:1 with RPMI+2mM Glutamine and cultured with ligands at 370 centigrade and 5% CO2 for six hours durations. Ligands used to stimulate specific population of cells at final concentrations were: soluble anti-CD3 (clone:OKT3) + anti-CD28 (clone: CD28.6) (10µg/ml each); phytohemagglutinin (PHA; 10µg/ml; Sigma-Aldrich); phorbol myristate acetate (PMA; 50ηg/ml; Sigma-Aldrich) + ionomycin (0.5µg/ml; Sigma-Aldrich) and R848 (5µg/ml; Invivogen). Brefeldin A (10µg/ml) was added after the first hour of culture to inhibit protein secretion for assays measuring intracellular cytokines. For cytokine measurement, supernatants were harvested immediately at the end of cell culture and stored at -20 degrees centigrade until analysis by multiplexed particle based flow cytometry assay on a Luminex analyzer (Bio-Plex, Bio-rad, UK). Samples from healthy volunteers were set up in parallel as positive controls.

Flow cytometry: Following flurochrome tagged anti-human monoclonal antibodies were obtained from BD biosciences (UK): anti-CD69 (cat#:555531), anti-CD45RA (cat#: 555488), anti-CD8 (cat#: 555369), anti-CD62L (cat#: 559772), anti-CD3 (cat#: 3010928), anti-TNFα (cat#: 559321), anti-CD123 (cat#: 560087), anti-CD19 (cat#: 339190), anti-CD14 (cat#: 560180), anti-CD11c (cat#: 560370), anti-HLA-DR (cat#: 347402), anti-IFNγ (cat#: 560741) and anti-CD4 (cat#:560251). Anti-human interferon α (PBL interferon source; 21112-3) and IL-17 (Ebiosciences; 11071-79-71) were obtained from other sources. A two-step staining process for surface and intracellular antigens was performed according to manufacturer instructions using BD fix-perm kit. Flow cytometry data were acquired on a BD FACS canto II. At least 200,000 events were collected for lymphocyte assays and 500,000 for the dendritic cell assays. Data were analyzed using FACS Diva software and gating strategy is illustrated in the figures S1a & S1b (1, 2).

Results:

In-vitro stimulation of PBMCs with T lymphocyte-specific stimuli led to T cell subsets expression of activation marker CD69 (Fig S2a) and interleukin-2 (IL-2) (Fig S2b) comparable to control. We analysed the terminal differentiation of CD4+ve T lymphocytes by enumeration of the TH1 (IFNγ producing) & TH17 (IL-17 producing) subsets in the patients. As shown in figure S2c, TH1 and TH17 development was similar to a control and within normal laboratory limits (data not shown). Similarly, CD8+ve and CD4-ve CD8-ve (double negative)

T lymphocytes produced IFNγ comparably to a healthy control on mitogen stimulation (Fig S2c). T cell subsets expressed memory markers in a similar pattern to healthy controls (Fig S2d). Taken together, these data suggest that although T lymphocyte numbers were low, T cell function was normal.

Figure legends:

Figure S1: Gating strategy S1a: Lymphocyte subsets. S2a: Antigen presenting cells. Monocytes : HLA-DR+ve CD14+ve; Myeloid DC : HLA-DR+ve CD14-ve CD19-ve CD11c+ve CD123-ve; Plasmacytoid DC:HLA DR+ve CD14-ve CD19-ve CD11c-ve CD123+ve.

Figure S2: In-vitro functional assessment of T-lymphocytes and antigen presenting cells (APCs). Patient A's responses were representative of patient B's responses where data is not shown. S2a. Patient A's T-lymphocyte subsets expressed activation marker CD69 comparably to a healthy control (CON). S2b. IL-2 production was comparable to a healthy control. S2c: Cytokine (IFNγ and IL-17) production by T-lymphocyte subsets was comparable to a healthy control (CON). S2d. Memory phenotyping of T-lymphocyte subsets was comparably to a healthy control (CON).

Figure S3: Delineation of break points of exon 13 deletion by Sanger sequencing of PCR products. Analysis was performed on the publicly available nucleotide blast program. (http://www.ncbi.nlm.nih.gov/BLAST/Blast.cgi?PAGE_TYPE=BlastSearch&BLAST_SPEC=OGP__9606__9558)

S3a: The 2350bps PCR product obtained (using primers EX13LF & EX13LR) from the mother aligned a one fragment against the reference sequence of MTHFD1 (arrow). S3b: The 600bps PCR product obtained (using primers EX13LF & EX13LR) from patient A aligned against the reference sequence of MTHFD1 (arrow) with a gap of 1745 bps confirming deletion that involves Exon 13.

Figure S4: Allele specific PCR. S4a: PCR conditions were set to exclude the 2350 bps product from the EX13LF and EX13LR primers. In this conditions PCR amplification of the patients showed two products of approximately 1500 and 600 bps. PCR amplification showed of the mother showed only one product of approximately 1500 bps as expected. S4b: Agarose gel electrophoresis of the allele specific PCR product from the patient A and mother demonstrating the heterozygous state.

Figure S5: Identification of an Alu-mediated deletion in MTHFD1. S5a: schematic representation of repetitive elements encompassing the deletion. Introns are shown as lines, exon 13 as a red rectangle, deletion as a blue

~~rectangle. Annotation of transposed elements is based on a reference sequence (hg19). S5b: sequence alignment of two AluS elements across the deletion breakpoint. Deleted nucleotides are in red.~~

~~Table S1.~~

~~Table S2a.~~

~~Table S2b.~~

~~Table S3a~~

~~Table S3b~~

~~Supplementary Fig 1~~

~~Supplementary Fig 2~~

~~Supplementary Fig 3a~~

~~Supplementary Fig 3b~~

Methods: allele specific PCR

In a heterozygous state with one allele carrying a deletion, PCR products of two sizes are anticipated. We were unable to demonstrate the undeleted allele in the patients with primers EX13LF & EX13LR despite varying PCR conditions. To demonstrate the heterozygous state in the patients, we used allele specific primer (EX13SF) that is predicted to anneal to the deleted region. We set the PCR conditions to exclude the longer product (2350 bps) by limiting the extension time. As shown in the supplementary figure 4a the PCR product from the primers EX13SF and EX13LR is possible only from the undeleted allele and is predicted to be around 1500 bps. With extension time limited to exclude the 2350 bps product, PCR product (from EX13LF & EX13LR) is only possible from the allele carrying exon 13 deletion and is expected to be of 600 bps size. As shown in the supplemental figure s4b, analysis by agarose gel electrophoresis of PCR products from patient A and the mother shows a heterozygous state for EX13 deletion in the patient.

Supplementary Fig 4a

Supplementary Fig 4b

AluS repeats as the mechanism for exon 13 deletion:

Following breakpoint identification, further analysis revealed that the deletion boundaries around exon 13 were within homologous positions of flanking, parallel, AluS repeats (supplementary figure 5a & 5b). Alu elements are short interspersed elements, of approximately 300 bp in length and derive their name from a single recognition site for the restriction enzyme AluI located near the middle of the Alu element. Alu elements have amplified in primate genomes through a RNA dependent mechanism termed retroposition and human chromosomes contain about 1,000,000 Alu copies, which equal 10% of the total genome (3, 4). Alu elements continue to amplify at a rate of 1 in 200 births and insertion of Alu elements contribute to approximately 0.1% of human genetic disorders. In addition to disease caused by insertion of Alu elements, their dispersion throughout the genome provides ample opportunity for unequal homologous recombination that can lead to deletion or insertion mutations and most often occur intrachromosomally (3). As illustrated (Fig S5a & S5b), these nearby low-complexity sequence regions likely permitted replication slippage to occur, excising the 1745 bp region; this has been previously observed as a pathogenic mutational mechanism in other genes, such as in *BRCA1* (6).

Supplementary Fig 5a and 5b

Figure legends:

Figure S1: Gating strategy S1a: Lymphocyte subsets. S2a: Antigen presenting cells. Monocytes : HLA DR+ve CD14+ve; Myeloid DC : HLA DR+ve CD14-ve CD19-ve CD11c+ve CD123-ve; Plasmacytoid DC:HLA DR+ve CD14-ve CD19-ve CD11c-ve CD123+ve.

Figure S2: In-vitro functional assessment of T lymphocytes and antigen presenting cells (APCs). Patient A's responses were representative of patient B's responses where data is not shown. S2a. Patient A's T lymphocyte subsets expressed activation marker CD69 comparably to a healthy control (CON). S2b. IL-2 production was comparable to a healthy control. S2c: Cytokine (IFNγ and IL-17) production by T lymphocyte subsets was comparable to a healthy control (CON). S2d. Memory phenotyping of T lymphocyte subsets was comparably to a healthy control (CON).

Figure S3: Delineation of break points of exon 13 deletion by Sanger sequencing of PCR products. Analysis was performed on the publicly available nucleotide blast program. (http://www.ncbi.nlm.nih.gov/BLAST/Blast.cgi?PAGE_TYPE=BlastSearch&BLAST_SPEC=OGP__9606__9558)

S3a: The 2350bps PCR product obtained (using primers EX13LF & EX13LR) from the mother aligned a one fragment against the reference sequence of MTHFD1 (arrow). S3b: The 600bps PCR product obtained (using primers EX13LF & EX13LR) from patient A aligned against the reference sequence of MTHFD1 (arrow) with a gap of 1745 bps confirming deletion that involves Exon 13.

Figure S4: Allele specific PCR. S4a: PCR conditions were set to exclude the 2350 bps product from the EX13LF and EX13LR primers. In this conditions PCR amplification of the patients showed two products of approximately 1500 and 600 bps. PCR amplification showed of the mother showed only one product of approximately 1500 bps as expected. S4b: Agarose gel electrophoresis of the allele specific PCR product from the patient A and mother demonstrating the heterozygous state.

Figure S5: Identification of an Alu-mediated deletion in MTHFD1. S5a: schematic representation of repetitive elements encompassing the deletion. Introns are shown as lines, exon 13 as a red rectangle, deletion as a blue rectangle. Annotation of transposed elements is based on a reference sequence (hg19). S5b: sequence alignment of two AluS elements across the deletion breakpoint. Deleted nucleotides are in red.

References

1. Blimkie D, Fortuno ES, 3rd, Thommai F, Xu L, Fernandes E, Crabtree J, et al. Identification of B cells through negative gating-An example of the MIFlowCyt standard applied. Cytometry Part A : the journal of the International Society for Analytical Cytology. 2010;77(6):546-51.
2. Jansen K, Blimkie D, Furlong J, Hajjar A, Rein-Weston A, Crabtree J, et al. Polychromatic flow cytometric high-throughput assay to analyze the innate immune response to Toll-like receptor stimulation. Journal of immunological methods. 2008;336(2):183-92.

3. Deininger PL, Batzer MA. Alu repeats and human disease. Molecular genetics and metabolism. 1999;67(3):183-93.

4. Rowold DJ, Herrera RJ. Alu elements and the human genome. Genetica. 2000;108(1):57-72.

5. Tancredi M, Sensi E, Cipollini G, Aretini P, Lombardi G, Di Cristofano C, et al. Haplotype analysis of BRCA1 gene reveals a new gene rearrangement: characterization of a 19.9 KBP deletion. European journal of human genetics : EJHG. 2004;12(9):775-7.

ON LINE REPOSITORY MATERIAL:

Precision molecular diagnosis defines specific therapy in combined immunodeficiency with megaloblastic anaemia secondary to *MTHFD1* deficiency.

Index:

Case Description

The first child (patient A) presented at 4 months of age with a two - week history of breathlessness, poor feeding and weight loss. His chest X-ray was consistent with *Pneumocystis Jirovecii* pneumonia (PCP), which was confirmed on bronchoalveolar lavage. He was suspected to have severe combined immunodeficiency (SCID) on the basis of lymphopenia ($0.9x\ 10^9$/L), which involved all the lymphoid subsets. HIV tests were negative and extensive investigations excluded all known SCID gene defects. Although he had T lymphopenia, he had normal distribution of subsets, T-cell- receptor (TCR) repertoire and his proliferation to phytohaemagglutinin (PHA) was comparable to control. A diagnosis of undefined SCID was made and he was listed for a hematopoietic stem cell transplant (HSCT). After his recovery from PCP, he was discharged home on cotrimoxazole, fluconazole and subcutaneous immunoglobulin (SCIG), awaiting a matched donor. Patient A was born to a South Asian mother and Caucasian father at 36+6 weeks gestation. His elder sister was reported to be healthy and there was no significant family history of immunodeficiency or metabolic disorders. The mother was known to carry hepatitis B virus. At 2 months of age, he was found to be anemic despite apparently thriving normally. Investigation for hemolytic anaemia was negative and symptoms resolved with folate and iron supplements for 2 weeks. HSCT was postponed despite finding a well-matched unrelated donor, as he remained clinically well with an improving immunological picture. Although he did not suffer significant infections, he remained lymphopenic and the evolving hypogammaglobulinemia led to reconsideration of HSCT. In the interim, his mother became pregnant and HSCT was postponed in view of his progress, the lack of ongoing opportunistic infections and a potential for getting a better donor match when the sibling was born.

His brother (patient B) was born when his elder sibling was 18 months old and displayed similar lymphopenia to his elder patient. He was started on fluconazole and cotrimoxazole prophylaxis soon after diagnosis, but IVIG was withheld to try to establish better immunological assessment. He was immunized with inactivated vaccines between 2 and 5 months according to the UK infant immunization programme. His immunoglobulin levels dropped below normal limits by the age of 6 months and although he responded to tetanus he did not respond to conjugated HiB vaccine (table s3b) and he was therefore started on azithromycin prophylaxis at 6 months of age. Subsequently he presented at 9 months of age with septic arthritis of his left hip. Blood culture and joint aspiration pus identified *Streptococcus pneumoniae*. While patient B was still hospitalized, patient A presented with a 1 week history of pallor and was found to be severely anemic (Hb 34 gms/L). Bone marrow examination

showed a marked megaloblastic picture. RBC folate and Vitamin B12 levels were within normal limits, therefore cotrimoxazole was considered to be a potential cause. Patient B also became anemic during the course of his septic arthritis treatment (Hb 6.4 gms/dl). Bone marrow examination performed at this time showed a megaloblastic picture and cotrimoxazole was discontinued. Both boys were treated with a two-week course of parenteral vitamin B12 & calcium folinate. Patient A was started on pentamidine nebulizers for PCP prophylaxis. Due to parental concern regarding medicalization and therapy safety, patient B was not given any PCP prophylaxis. Patient B was started on subcutaneous immunoglobulin therapy at 10 months of age. Despite this, patient B suffered further pyogenic infections that included pneumonia (organism not isolated) at 19 months, peri-orbital cellulitis at 22 months and pneumococcal bacteremia at 24 months. The infection at 19 months of age was accompanied by a further episode of megaloblastic anemia.

Immunological evaluations revealed that both patients were lymphopenic for all subsets throughout their follow up (Table S2a & S2b). Both patients had low IgM levels whilst on immunoglobulin replacement therapy suggestive of antibody deficiency. Patient A was not immunized in infancy whilst patient B was vaccinated with inactive vaccines and showed adequate tetanus titers but did not develop protective HiB titers (Table S3b).

T cell subsets expressed memory markers in a pattern similar to healthy controls (data shown in main article). T cell subsets expressed activation marker CD69 in response to TCR specific stimuli (data shown in main article). T helper subset enumeration showed comparable numbers of TH1 & TH17 development (data shown in main article). Both siblings continued to have normal T cell proliferation, but their T cell receptor excision circle (TREC) counts remained low suggestive of low thymic output. Following the initiation of calcium folinate supplementation both patients have remained free of infections and have mounted protective vaccine responses following the cessation of immunoglobulin replacement therapy (Table S3a & S3b). Both patients are in regular schools with no disabilities identified. Both had normal MRI brain and plasma/CSF folate studies before regular folinic acid supplements were started. Following their successful treatment and identification of the molecular cause the family have been informed that HSCT is no longer a therapeutic consideration.

Immunological experiments

Methods:

Cell culture: Lithium heparin anticoagulated blood samples were obtained from the patients and experiments were set up within 4 hours of sampling. Whole blood was diluted 1:1 with RPMI+2mM Glutamine and cultured with ligands at 370 centigrade and 5% CO2 for six hours durations. Ligands used to stimulate specific population of cells at final concentrations were: soluble anti-CD3 (clone:OKT3) + anti-CD28 (clone: CD28.6) (10µg/ml each); phytohemagglutinin (PHA; 10µg/ml; Sigma-Aldrich); phorbol myristate acetate (PMA; 50ηg/ml; Sigma-Aldrich) + ionomycin (0.5µg/ml; Sigma-Aldrich) and R848 (5µg/ml; Invivogen). Brefeldin A (10µg/ml) was added after the first hour of culture to inhibit protein secretion for assays measuring intracellular cytokines. For cytokine measurement, supernatants were harvested immediately at the end of cell culture and stored at -20 degrees centigrade until analysis by multiplexed particle based flow cytometry assay on a Luminex analyzer (Bio-Plex, Bio-rad, UK). Samples from healthy volunteers were set up in parallel as positive controls.

Flow cytometry: Following flurochrome tagged anti-human monoclonal antibodies were obtained from BD biosciences (UK): anti-CD69 (cat#:555531), anti-CD45RA (cat#: 555488), anti-CD8 (cat#: 555369), anti-CD62L (cat#: 559772), anti-CD3 (cat#: 3010928), anti-TNFα (cat#: 559321), anti-CD123 (cat#: 560087), anti-CD19 (cat#: 339190), anti-CD14 (cat#: 560180), anti-CD11c (cat#: 560370), anti-HLA-DR (cat#: 347402), anti-IFNγ (cat#: 560741) and anti-CD4 (cat#:560251). Anti-human interferon α (PBL interferon source; 21112-3) and IL-17 (Ebiosciences; 11071-79-71) were obtained from other sources. A two-step staining process for surface and intracellular antigens was performed according to manufacturer instructions using BD fix-perm kit. Flow cytometry data were acquired on a BD FACS canto II. At least 200,000 events were collected for lymphocyte assays and 500,000 for the dendritic cell assays. Data were analyzed using FACS Diva software and gating strategy is illustrated in the figures S1a & S1b (1, 2).

Results:

In-vitro stimulation of PBMCs with T lymphocyte-specific stimuli led to T cell subsets expression of activation marker CD69 (Fig S2a) and interleukin-2 (IL-2) (Fig S2b) comparable to control. We analysed the terminal differentiation of CD4+ve T lymphocytes by enumeration of the TH1 (IFNγ producing) & TH17 (IL-17 producing) subsets in the patients. As shown in figure S2c, TH1 and TH17 development was similar to a control and within normal laboratory limits (data not shown). Similarly, CD8+ve and CD4-ve CD8-ve (double negative)

T lymphocytes produced IFNγ comparably to a healthy control on mitogen stimulation (Fig S2c). T cell subsets expressed memory markers in a similar pattern to healthy controls (Fig S2d). Taken together, these data suggest that although T lymphocyte numbers were low, T cell function was normal.

Methods: allele specific PCR

In a heterozygous state with one allele carrying a deletion, PCR products of two sizes are anticipated. We were unable to demonstrate the undeleted allele in the patients with primers EX13LF & EX13LR despite varying PCR conditions. To demonstrate the heterozygous state in the patients, we used allele specific primer (EX13SF) that is predicted to anneal to the deleted region. We set the PCR conditions to exclude the longer product (2350 bps) by limiting the extension time. As shown in the supplementary figure 4a the PCR product from the primers EX13SF and EX13LR is possible only from the undeleted allele and is predicted to be around 1500 bps. With extension time limited to exclude the 2350 bps product, PCR product (from EX13LF & EX13LR) is only possible from the allele carrying exon 13 deletion and is expected to be of 600 bps size. As shown in the supplemental figure s4b, analysis by agarose gel electrophoresis of PCR products from patient A and the mother shows a heterozygous state for EX13 deletion in the patient.

Supplementary Fig 4a

Supplementary Fig 4b

AluS repeats as the mechanism for exon 13 deletion:

Following breakpoint identification, further analysis revealed that the deletion boundaries around exon 13 were within homologous positions of flanking, parallel, AluS repeats (supplementary figure 5a & 5b). Alu elements are short interspersed elements, of approximately 300 bp in length and derive their name from a single recognition site for the restriction enzyme AluI located near the middle of the Alu element. Alu elements have amplified in primate genomes through a RNA dependent mechanism termed retroposition and human chromosomes contain about 1,000,000 Alu copies, which equal 10% of the total genome (3, 4). Alu elements continue to amplify at a rate of 1 in 200 births and insertion of Alu elements contribute to approximately 0.1% of human genetic disorders. In addition to disease caused by insertion of Alu elements, their dispersion throughout the genome provides ample opportunity for unequal homologous recombination that can lead to deletion or insertion mutations and most often occur intrachromosomally (3). As illustrated (Fig S5a & S5b),

these nearby low-complexity sequence regions likely permitted replication slippage to occur, excising the 1745 bp region; this has been previously observed as a pathogenic mutational mechanism in other genes, such as in *BRCA1* (6).

Supplementary Fig 5a and 5b

Figure legends:

Figure S1: Gating strategy S1a: Lymphocyte subsets. S2a: Antigen presenting cells. Monocytes : HLA DR+ve CD14+ve; Myeloid DC : HLA DR+ve CD14-ve CD19-ve CD11c+ve CD123-ve; Plasmacytoid DC:HLA DR+ve CD14-ve CD19-ve CD11c-ve CD123+ve.

Figure S2: In-vitro functional assessment of T lymphocytes and antigen presenting cells (APCs). Patient A's responses were representative of patient B's responses where data is not shown. S2a. Patient A's T lymphocyte subsets expressed activation marker CD69 comparably to a healthy control (CON). S2b. IL-2 production was comparable to a healthy control. S2c: Cytokine (IFNγ and IL-17) production by T lymphocyte subsets was comparable to a healthy control (CON). S2d. Memory phenotyping of T lymphocyte subsets was comparably to a healthy control (CON).

Figure S3: Delineation of break points of exon 13 deletion by Sanger sequencing of PCR products. Analysis was performed on the publicly available nucleotide blast program. (http://www.ncbi.nlm.nih.gov/BLAST/Blast.cgi?PAGE_TYPE=BlastSearch&BLAST_SPEC=OGP__9606__9558)

S3a: The 2350bps PCR product obtained (using primers EX13LF & EX13LR) from the mother aligned a one fragment against the reference sequence of MTHFD1 (arrow). S3b: The 600bps PCR product obtained (using primers EX13LF & EX13LR) from patient A aligned against the reference sequence of MTHFD1 (arrow) with a gap of 1745 bps confirming deletion that involves Exon 13.

Figure S4: Allele specific PCR. S4a: PCR conditions were set to exclude the 2350 bps product from the EX13LF and EX13LR primers. In this conditions PCR amplification of the patients showed two products of approximately 1500 and 600 bps. PCR amplification showed of the mother showed only one product of

approximately 1500 bps as expected. S4b: Agarose gel electrophoresis of the allele specific PCR product from the patient A and mother demonstrating the heterozygous state.

Figure S5: Identification of an Alu-mediated deletion in MTHFD1. S5a: schematic representation of repetitive elements encompassing the deletion. Introns are shown as lines, exon 13 as a red rectangle, deletion as a blue rectangle. Annotation of transposed elements is based on a reference sequence (hg19). S5b: sequence alignment of two AluS elements across the deletion breakpoint. Deleted nucleotides are in red.

Table S1.

Table S2a.

Table S2b.

Table S3a

Table S3b

Supplementary Fig 1

Supplementary Fig 2

Supplementary Fig 3a

Supplementary Fig 3b

References

1. Blimkie D, Fortuno ES, 3rd, Thommai F, Xu L, Fernandes E, Crabtree J, et al. Identification of B cells through negative gating-An example of the MIFlowCyt standard applied. Cytometry Part A : the journal of the International Society for Analytical Cytology. 2010;77(6):546-51.
2. Jansen K, Blimkie D, Furlong J, Hajjar A, Rein-Weston A, Crabtree J, et al. Polychromatic flow cytometric high-throughput assay to analyze the innate immune response to Toll-like receptor stimulation. Journal of immunological methods. 2008;336(2):183-92.

3. Deininger PL, Batzer MA. Alu repeats and human disease. Molecular genetics and metabolism. 1999;67(3):183-93.

4. Rowold DJ, Herrera RJ. Alu elements and the human genome. Genetica. 2000;108(1):57-72.

5. Tancredi M, Sensi E, Cipollini G, Aretini P, Lombardi G, Di Cristofano C, et al. Haplotype analysis of BRCA1 gene reveals a new gene rearrangement: characterization of a 19.9 KBP deletion. European journal of human genetics : EJHG. 2004;12(9):775-7.

Figure No. 1

Click here to download high resolution image

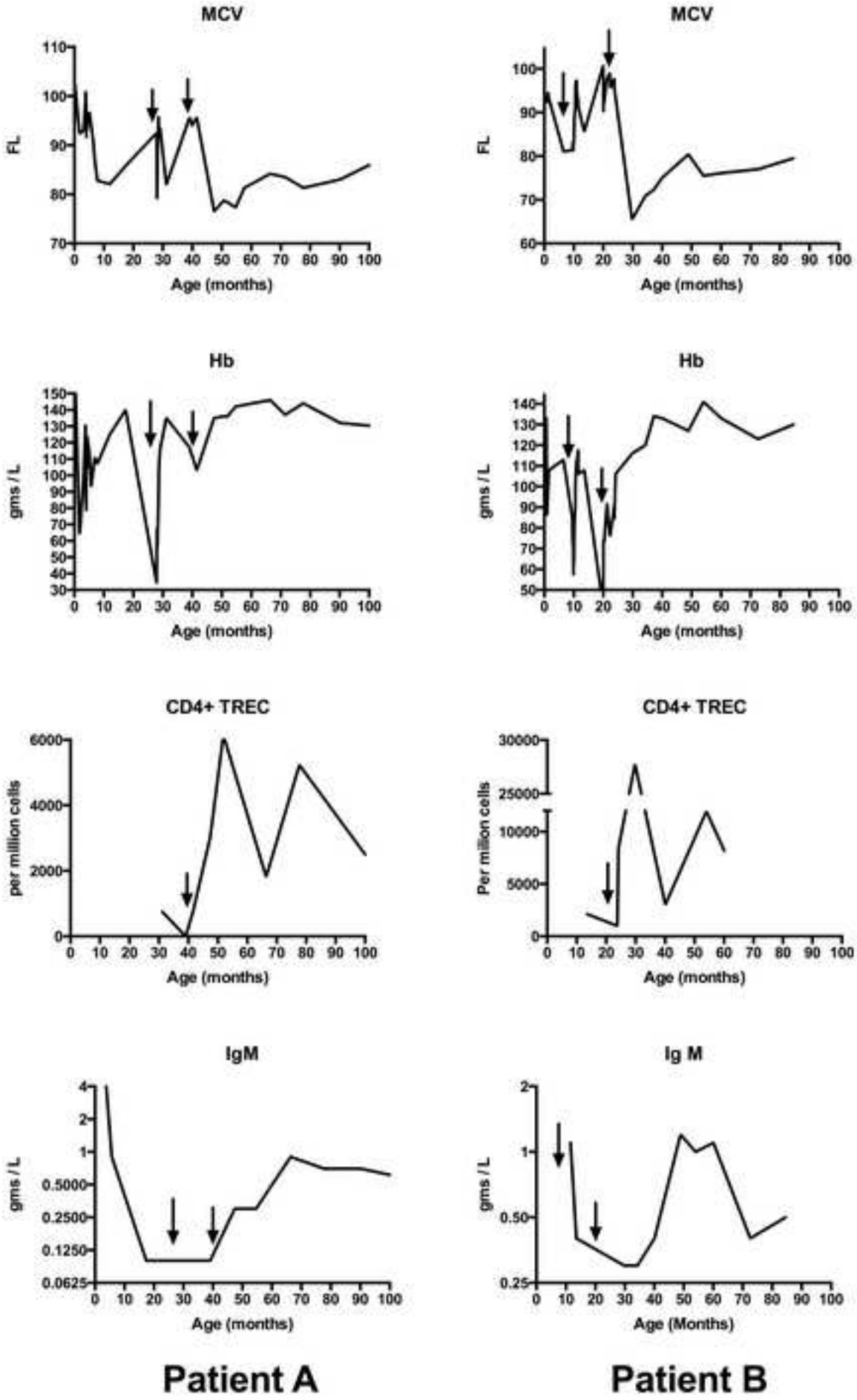

Figure No. 2a

Click here to download high resolution image

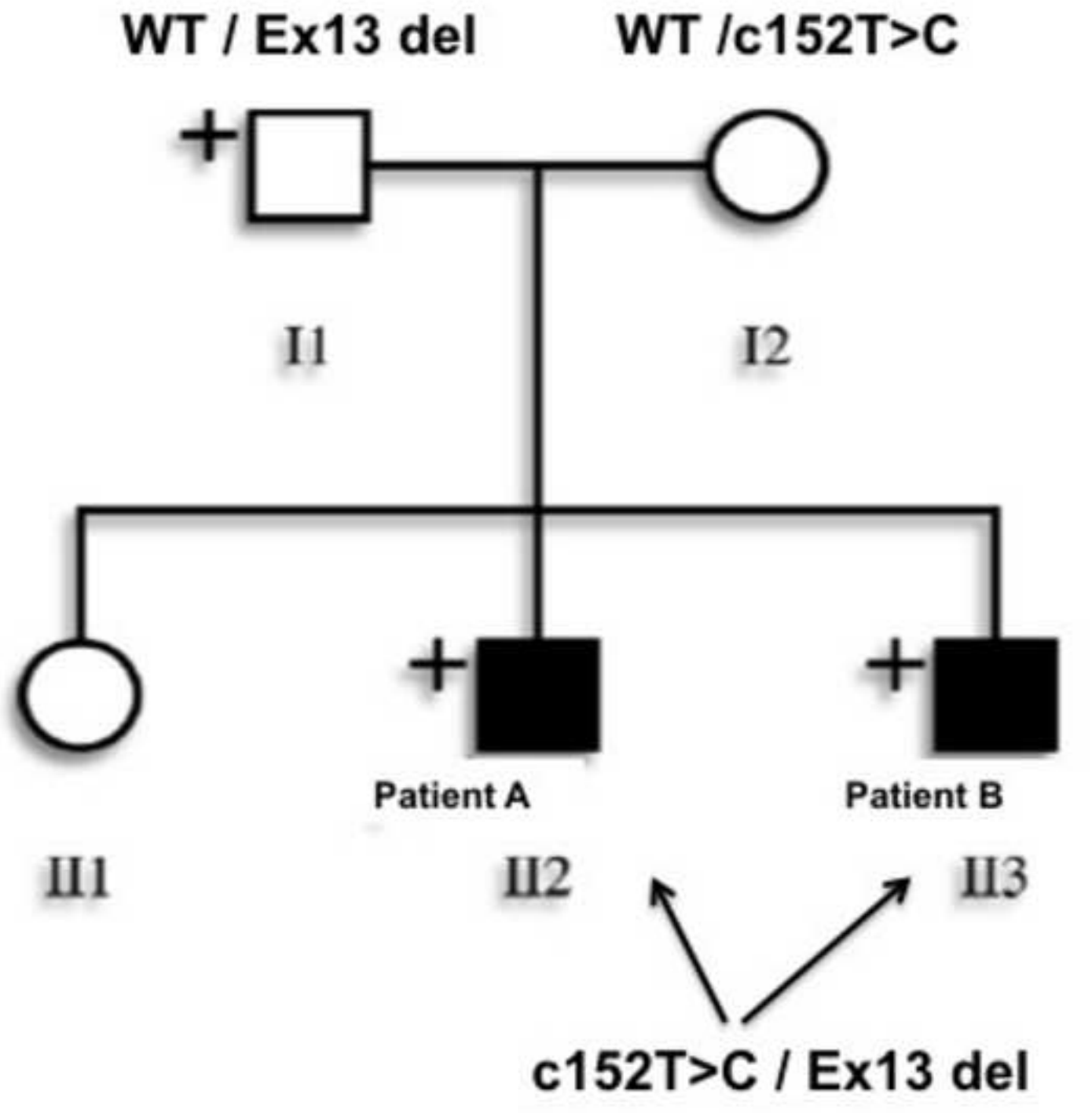

Figure No. 2b

Click here to download high resolution image

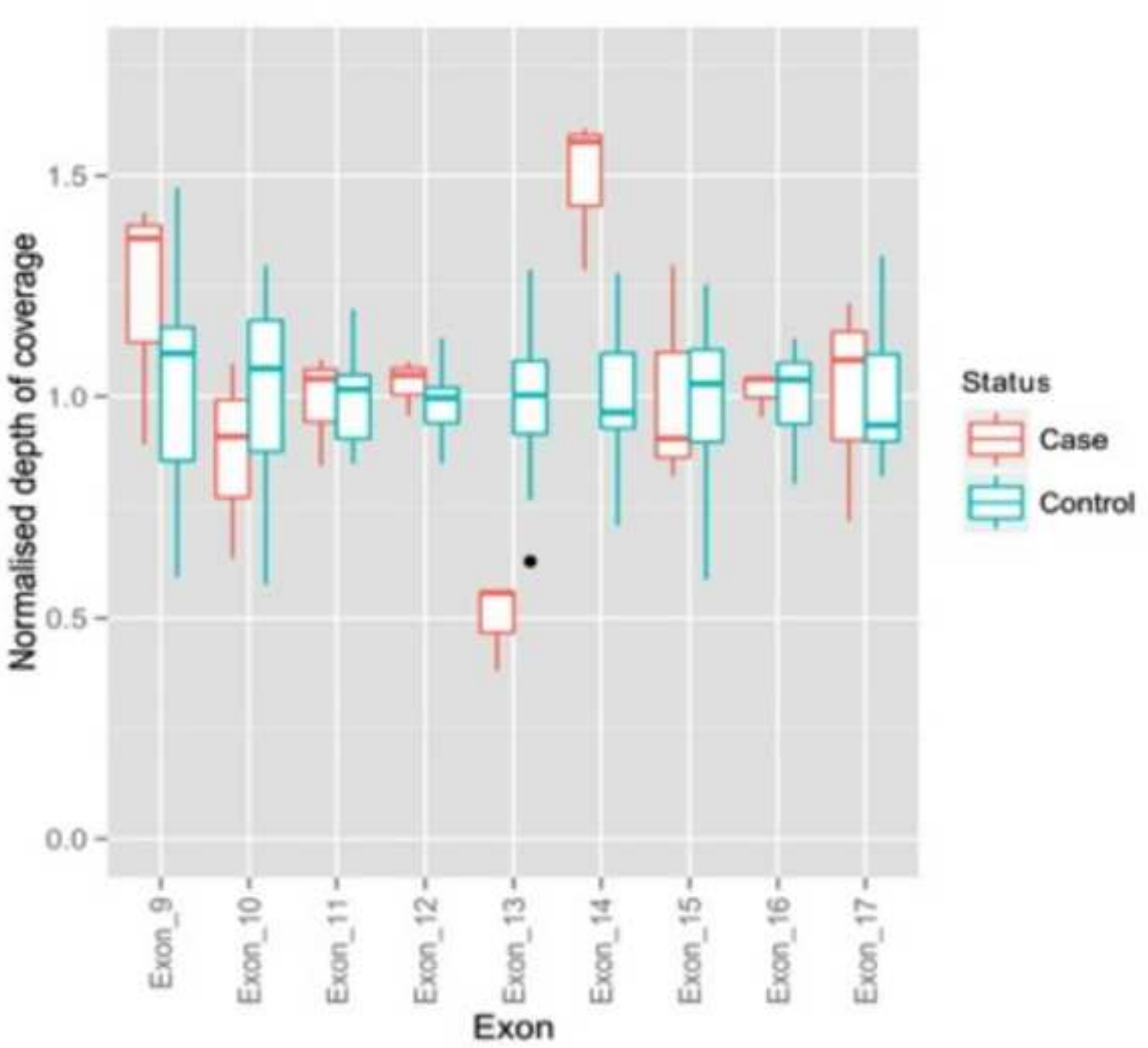

Figure No. 2c

Click here to download high resolution image

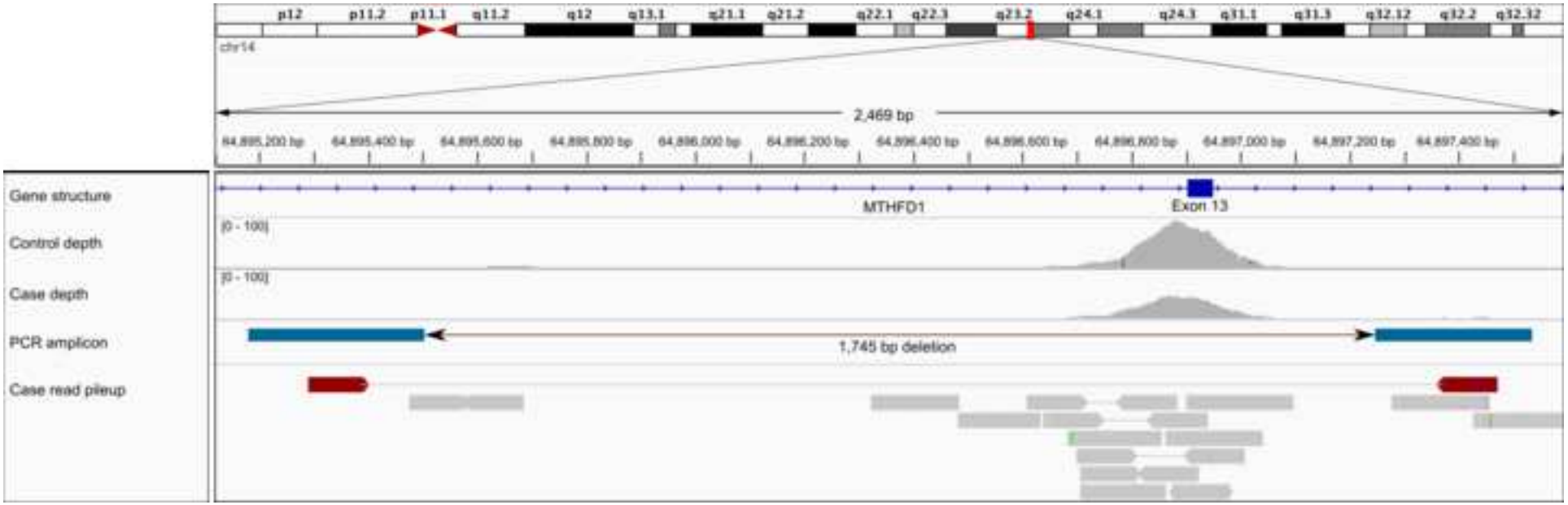

Figure No. 2d

Click here to download high resolution image

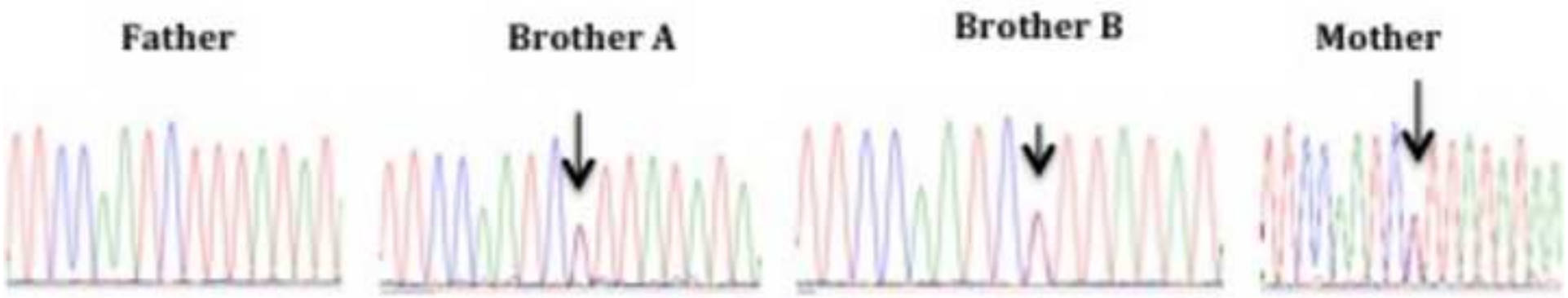

Figure No. 2e

Click here to download high resolution image

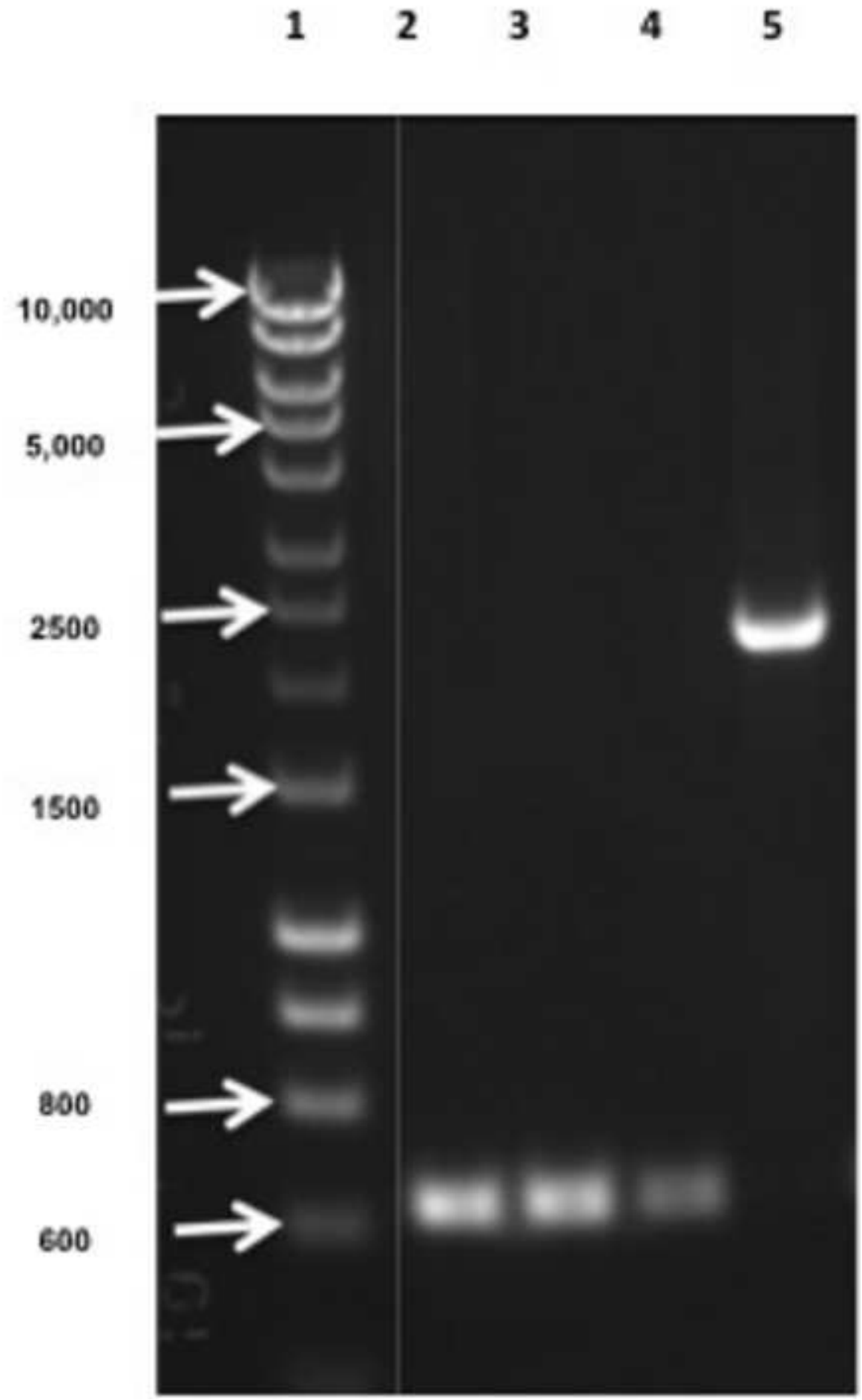

Repository E Figure No. 1a

Click here to download high resolution image

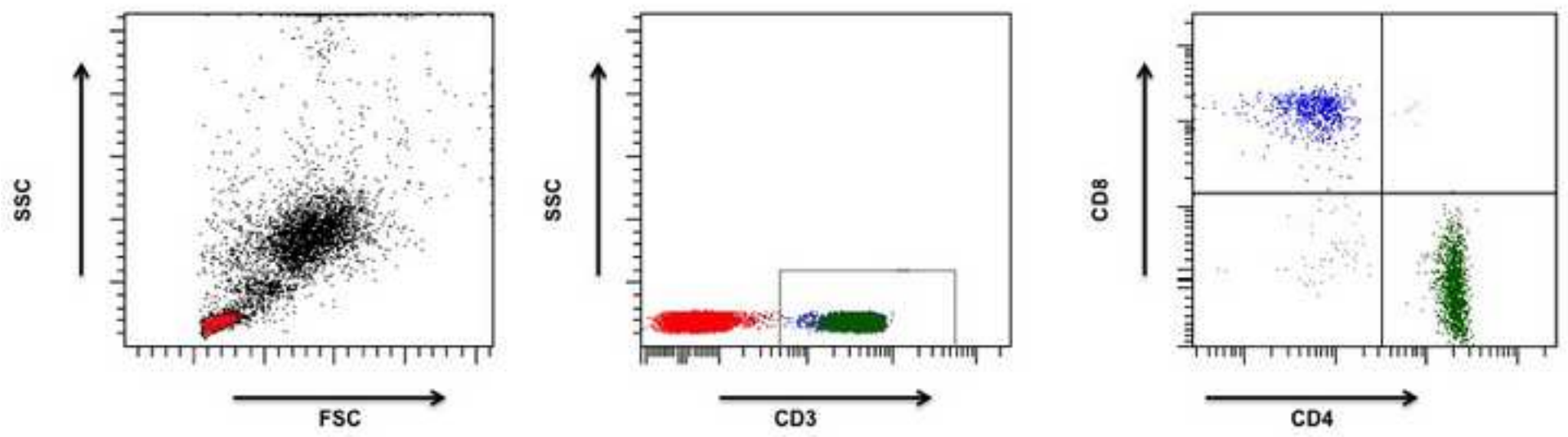

Repository E Figure No. 1b

Click here to download high resolution image

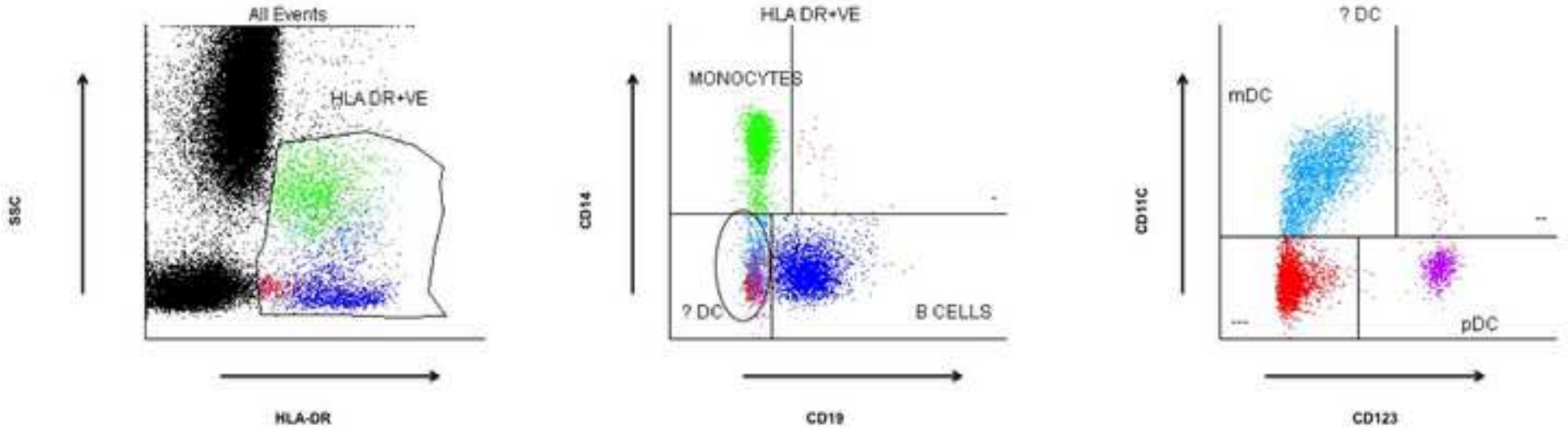

Repository E Figure No. 2a

Click here to download high resolution image

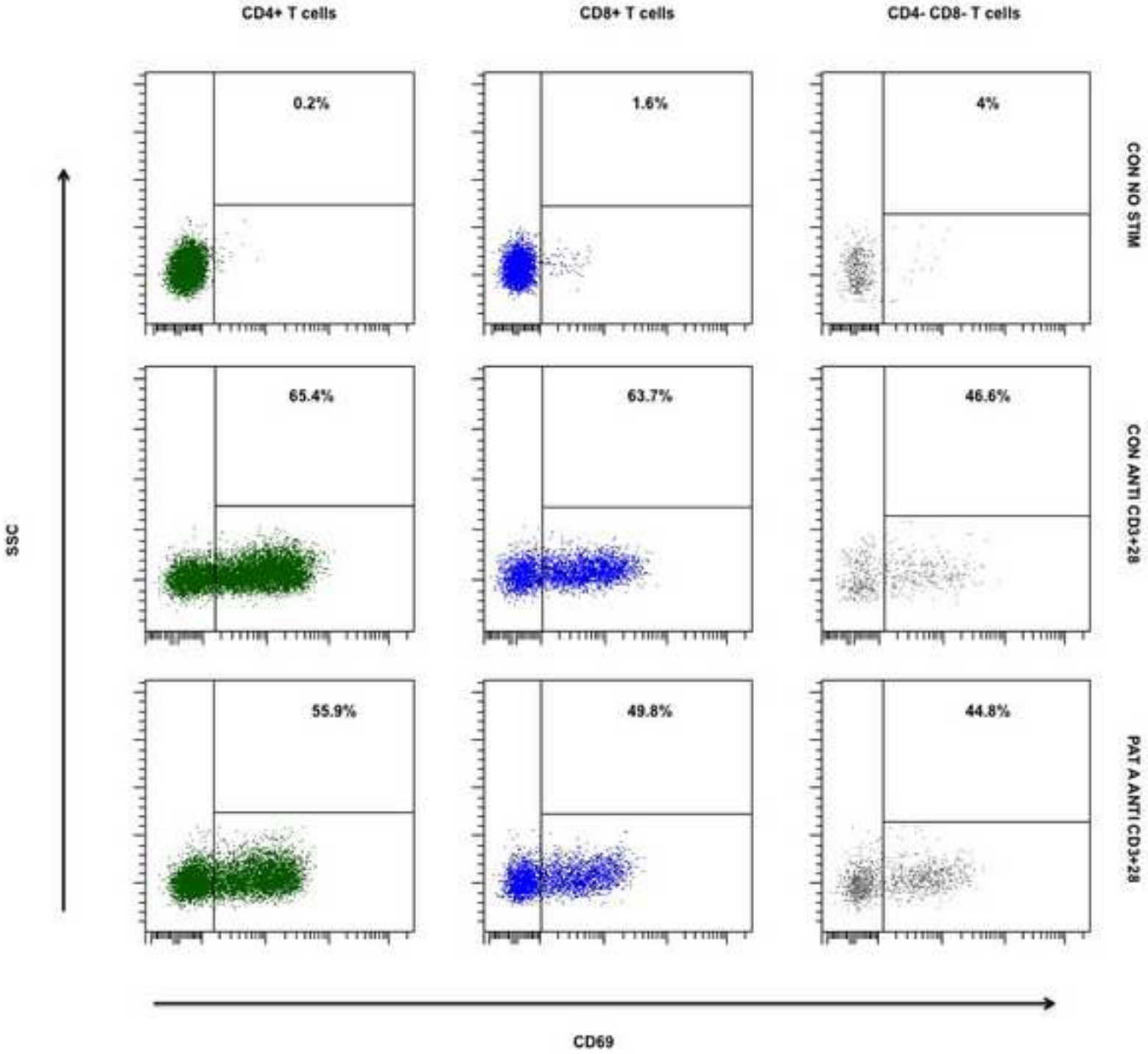

Repository E Figure No. 2b
Click here to download high resolution image

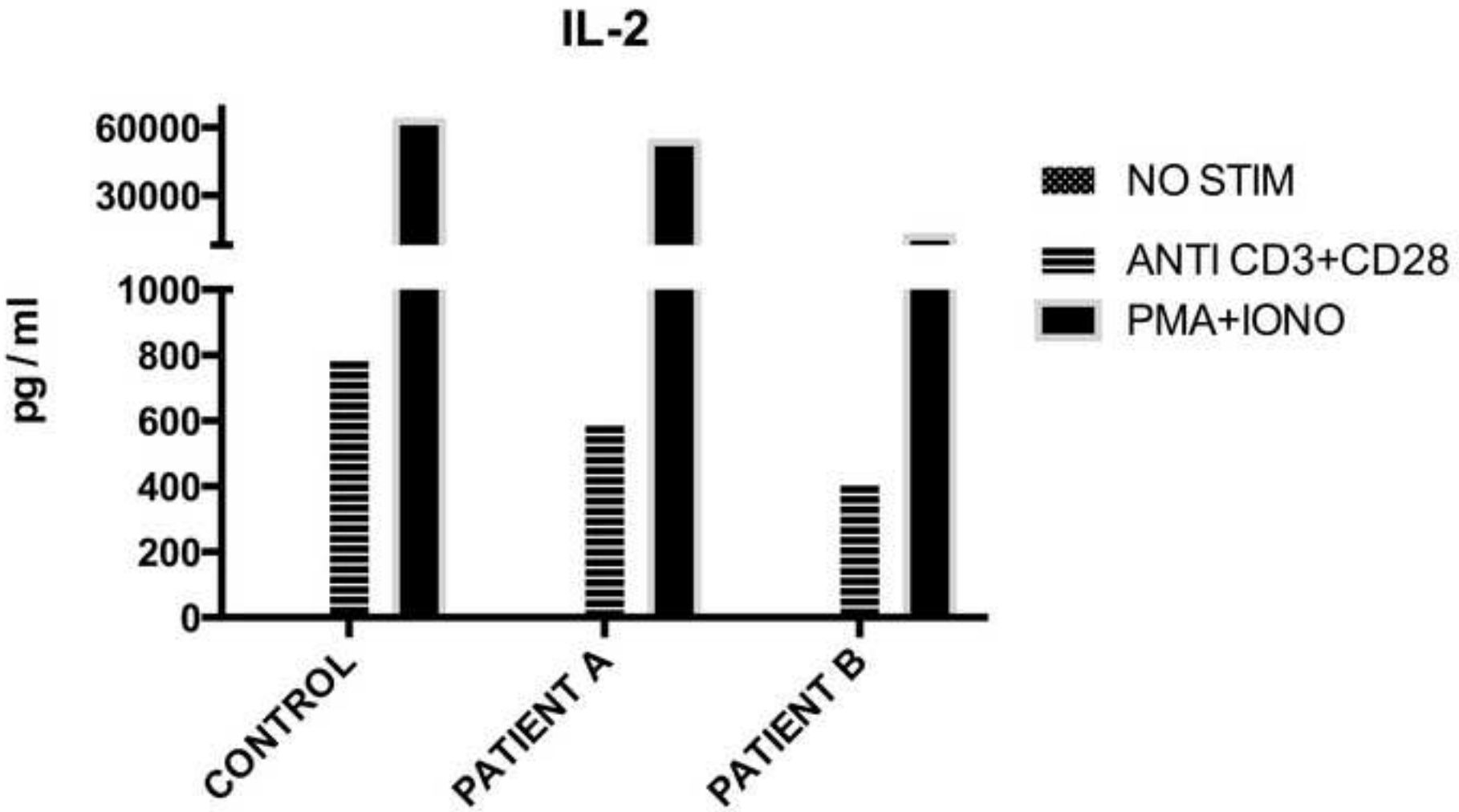

Repository E Figure No. 2c

Click here to download high resolution image

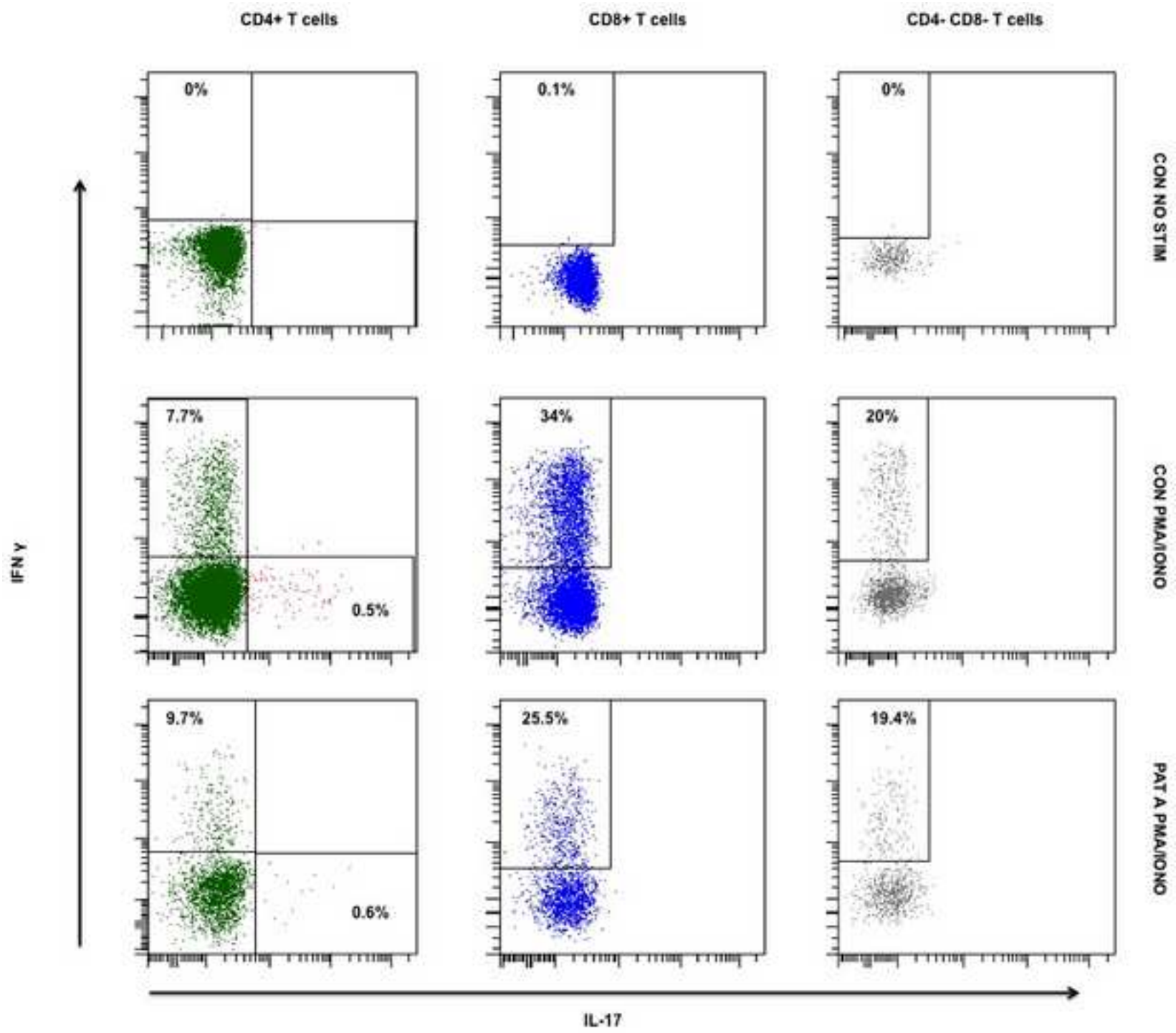

Repository E Figure No. 2d

Click here to download high resolution image

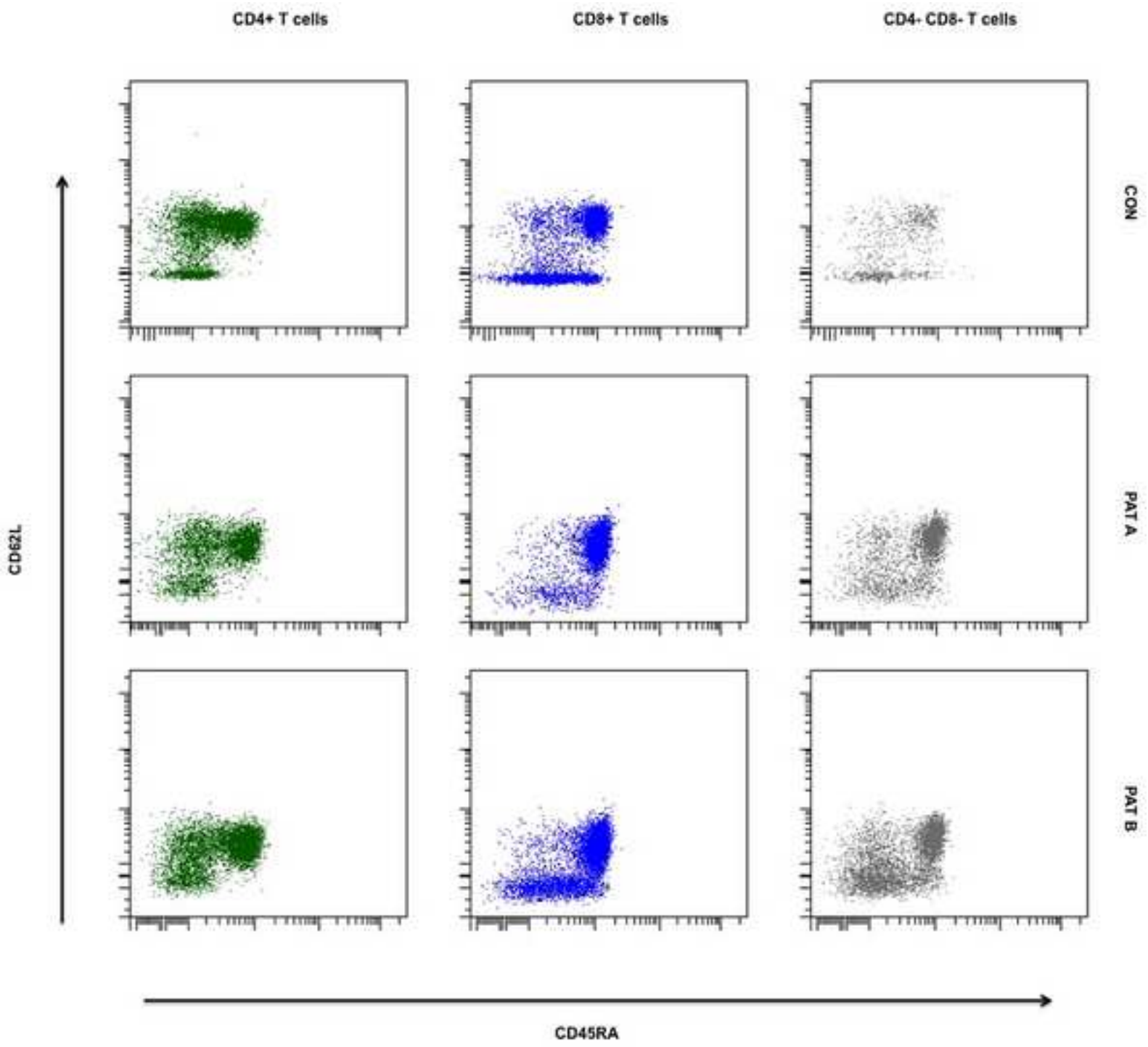

Repository E Figure No. 3a

Click here to download high resolution image

Homo sapiens methylenetetrahydrofolate dehydrogenase (NADP+ dependent) 1, methenyltetrahydrofolate cyclohydrolase, formyltetrahydrofolate synthetase (MTHFD1), RefSeqGene on chromosome 14

NCBI Reference Sequence: NG_012450.1

GenBank FASTA

Repository E Figure No. 3b

Click here to download high resolution image

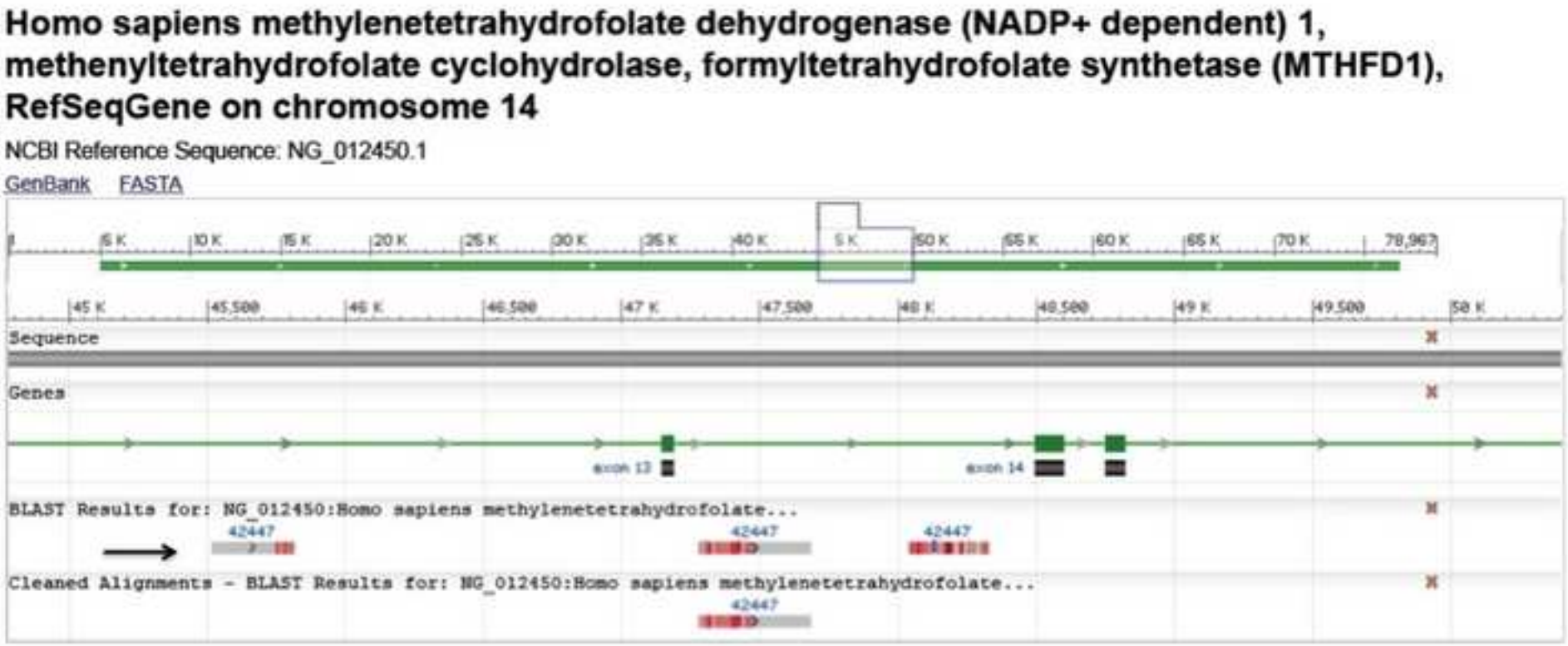

Repository E Figure No. 4a

Click here to download high resolution image

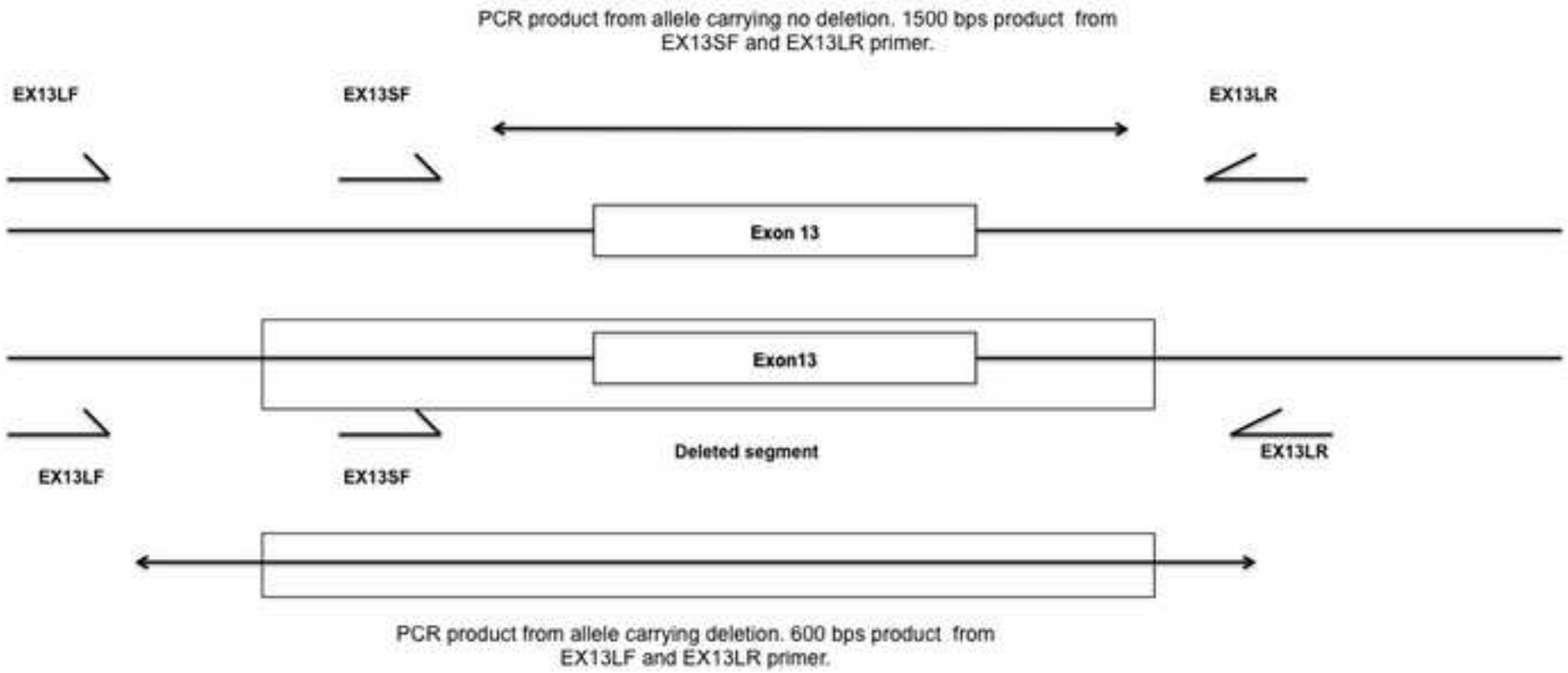

Repository E Figure No. 4b

Click here to download high resolution image

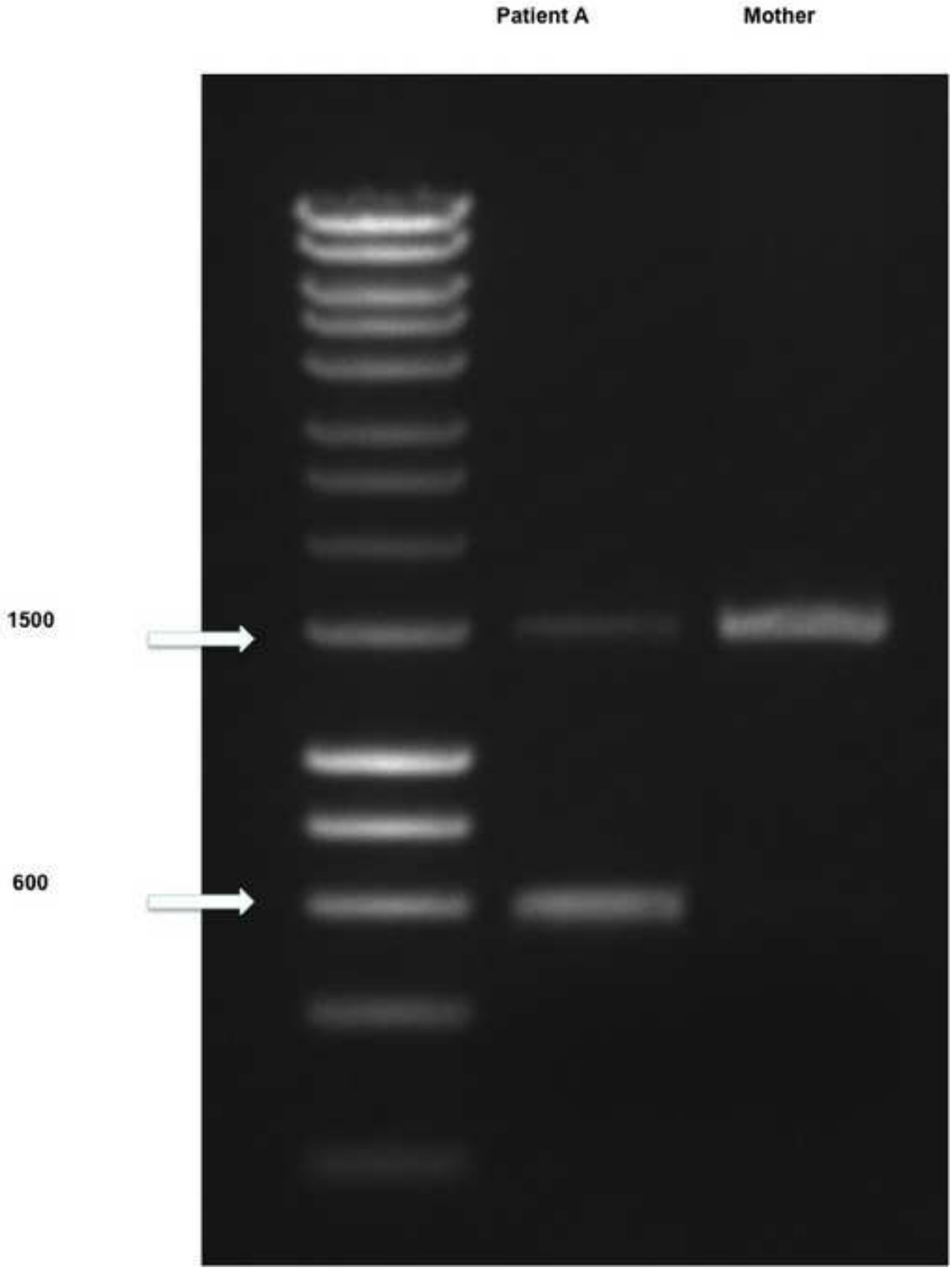

Repository E Figure No. 5
Click here to download high resolution image

A

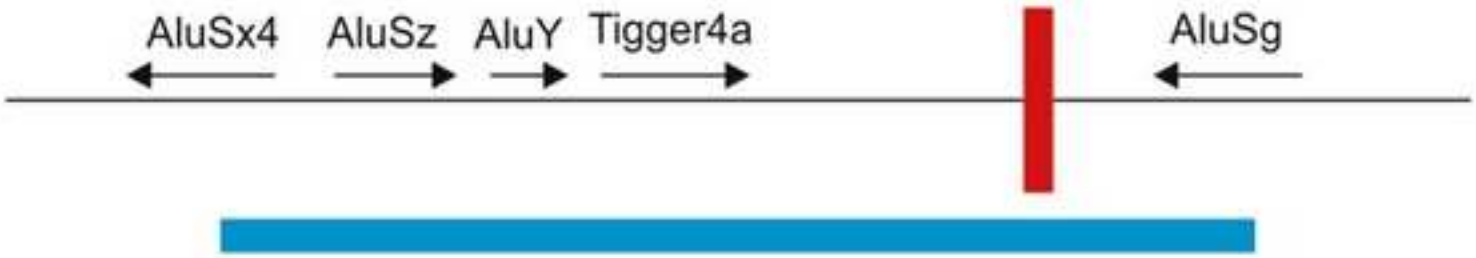

B

```
AluSx4  GGAGACACAGTCTCGCTCTGTTGCCTGG-GCTGGAGTACAGTGGCACGATCTTGGCTCAC 59
AluSg   ---GACGGAGTCTTGCTCTGTTGCCCAGAGCTGGAGTGCAATGGCGCAATCTCGGCTCAC 57
           ***  ***** ***********  * ******** ** **** * **** *******

AluSx4  TGCAACCTCCGCCTCCTGGTTTCAAGCAATTCTCCTGCCTCAGCCTCCCAAGTAGCTGGG 119
AluSg   TGCAACCTCTGCCTCCCAGGTTCAAGCAACTCTCCTGCGTCAGCCTCCCGAGTAGCTGGG 117
        ********* ******  * ********* ******** ********** **********

AluSx4  ACTACAGGTGCGTGCCACCATGCCTGGCTAATTTTTGTGTTTTTAGTAGAGATGGGGTTT 179
AluSg   ATTACAGGCATGCACCACCACGCTCAGCTAATTTT-GTATTTTTAGTAGAGACGGGGTTT 176
        * ******   *  ****** **   ********** ** ************** *******

AluSx4  CACTATATTGGCCAGGCTGGTCTTGAACTCCTGACCTTGTGATCTGCCCACCTTGGCCTC 239
AluSg   CACCGTGTTGGCCAAGCTGGTCTTGAACTCCTGACCTCGTGATCCGCCCACCTCGGCCTC 236
        ***  * ******* ************************ ****** ******** ******

AluSx4  CCAATGTGCTGGGATAATAGGCATGAGCCACCGTGCCCAGCC 281
AluSg   CCAAAGTGCTGGTATTATAGGCGTGAGCCACCGCACCCAGCC 278
        **** ******* ** ****** **********  *******
```

Figure No. 2f

Click here to download high resolution image